

The macroecology behind macroevolution: North American
mammal functional diversity and its relation to environmental
change

Peter D. Smits^{1,*}

1. University of California – Berkeley, California, 94720.

* Corresponding author; e-mail: psmits@berkeley.edu.

Manuscript elements:

Keywords: macroecology, macroevolution, paleobiology, species pool, community assembly

Manuscript type: Article

Prepared using the suggested L^AT_EX template for *Am. Nat.*

Abstract

The set of species in a region changes over time as new species enter through speciation or immigration and as species leave the system through extinction and extirpation. How a regional species pool changes over time is the product of many processes acting at multiple levels of organization. Changes in the functional composition of a regional species pool are changes that occur across all local communities drawn from that species pool. While a species' presence in a local community is due to the availability of the necessary biotic-biotic or biotic-abiotic interactions that enable coexistence, a species' presence in a regional species pool just requires that at least one local community has that set of necessary interactions. The goal of this analysis is to understand when, and possibly for what reasons, mammal ecotypes are enriched or depleted relative to their average diversity. Here, I analyze the diversity history of North American mammals ecotypes for most of the Cenozoic (the last 65 million years). This analysis frames mammal diversity in terms of both their means of interacting with the biotic and abiotic environment (i.e. functional group or ecotype) as well as their regional and global environmental context. Using two hierarchical Bayesian hidden Markov models of diversity, I find that changes to mammal diversity are driven more by the influx of new species than by selective extinction. I also find that the only ecotypes which experience a near constant increase in diversity over time are digitigrade and unguligrade herbivores, while arboreal ecotypes become increasingly rare and in many cases disappear entirely from the species pool over the Cenozoic. Additionally, I find that global temperature is only associated with the origination of some mammal ecotypes but, in almost all cases, does not affect the extinction of mammal ecotypes.

Introduction

Changes to species diversity are the result of evolutionary and ecological processes acting in concert and continually over time. Local communities are shaped by dispersal and local ecological processes such as resource competition and predator-prey relationships. The constituent species of these communities are drawn from a regional species pool, or the set of all species that are present in at least one community within a region (Harrison and Cornell, 2008; Mittelbach and Schemske, 2015; Urban et al., 2008). Species dispersal from the regional species pool to the local communities is a

sorting process shaped by biotic and abiotic environmental filters which are mediated by those
30 species' traits (Cottenie, 2005; Elith and Leathwick, 2009; Harrison and Cornell, 2008; Loeuille and
Leibold, 2008; Shipley et al., 2006; Urban et al., 2008). Regional species pools are shaped by
32 speciation, extinction, migration, and extirpation. The gain or loss of regional diversity is the result
of macroevolutionary dynamics which, in turn, shape the downstream macroecological dynamics of
34 the regional species pool and its constituent local communities (Harrison and Cornell, 2008;
Mittelbach and Schemske, 2015; Urban et al., 2008). In turn, the distribution of species within
36 regional species pool represents the expected distribution of local communities under a purely
diffusive process of community assembly as would be expected neutral theory of biodiversity
38 CITATION.

Fundamentally, all species respond differently to climate and environmental change (Blois and
40 Hadly, 2009). Those species with similar ecological roles within a regional species pool can be
described as belonging to a guild or functional group (Bambach, 1977; Brown and Maurer, 1989;
42 Simberloff and Dayan, 1991; Valentine, 1969; Wilson, 1999). Species within the same functional
group are expected to have more similar macroecological dynamics to each other than to species of
44 a different functional group. By focusing on the relative diversity of functional groups, changes to
diversity are interpretable as changes to the set of ways species within a species pool could interact
46 with the biotic and abiotic environment.

A key question when comparing communities or regional species pools based on their functional
48 composition is whether specific functional groups are enriched or depleted and why; what are the
processes that led to a species pool having the functional composition it does (Blois and Hadly,
50 2009; Brown and Maurer, 1989; McGill et al., 2006; Smith et al., 2008; Weber et al., 2017)?

Comparisons of contemporaneous regional species pools can only determine if a functional group is
52 enriched or depleted in one species pool relative to the other species pools CITATION. These types
of comparison do not take into account if a functional group is enriched or depleted relative to its
54 diversity over time (Blois and Hadly, 2009). While a species pool may be depleted of a functional
group relative to other contemporaneous species pools, that same functional group may be actually
56 be enriched in that species pool relative to its historical diversity. Because the processes which

shape regional species pool diversity (e.g. origination, extinction) operate on much longer time scales than is possible for studies of the Recent, paleontological data provides a unique opportunity to observe and estimate the changes to functional diversity and how species functional traits and environmental context can shape the enrichment or depletion of functional groups within a regional species pool (Blois and Hadly, 2009; Smith et al., 2008). Being able to identify if the diversity of a functional group is depleted relative to their long term average diversity in the species pool is particularly useful in conservation settings; species in depleted groups are most likely more at risk of extinction than species in enriched groups, even if those enriched groups are relatively rare when compared to the functional composition of other contemporaneous species pools.

The paleontological record of North American mammals for the Cenozoic (\sim 66 million years ago to the present) provides one of the best opportunities for understanding how regional species pool functional diversity changes over time. The North American mammal record is a relatively complete temporal sequence for the entire Cenozoic which is primarily, but not exclusively, based on fossil localities from the Western Interior of North America (Alroy, 1996, 2009; Alroy et al., 2000). Additionally, mammal fossils preserve a lot of important physiological information, such as teeth, so that functional traits like the dietary/trophic category of species are easy to estimate (Eronen et al., 2010; Polly et al., 2011, 2015).

The goals of this study are to understand when are unique functional groups enriched or depleted in the North American mammal regional species pool and to estimate the relationship between these changes to regional ecotypic diversity and changes to their environmental context. My contribution is to develop a joint model of observation, origination, survival, as well as the effects of species traits and environmental factors on these processes.

Background

The history of standing diversity for all mammals along with that some individual clades of North American mammals for the Cenozoic has been the focus of considerable study (Alroy, 1996, 2009; Alroy et al., 2000; Badgley and Finarelli, 2013; Blois and Hadly, 2009; Figueirido et al., 2012;

Fraser et al., 2015; Janis, 1993; Janis and Wilhelm, 1993; Pires et al., 2015; Quental and Marshall, 84 2013; Silvestro et al., 2015; Slater, 2015; Smits, 2015). Previous approaches to understanding mammal diversity, both in North America and elsewhere, fall into a number of overlapping 86 categories: total diversity (Alroy, 1996; Alroy et al., 2000; Figueirido et al., 2012; Liow et al., 2008), with/between guild comparisons (Janis et al., 2004; Janis, 2008; Janis et al., 2000; Janis and 88 Wilhelm, 1993; Jernvall and Fortelius, 2004; Pires et al., 2015), within/between clade comparisons (Cantalapiedra et al., 2017; Fraser et al., 2015; Quental and Marshall, 2013; Silvestro et al., 2015; 90 Slater, 2015), and estimating the impact of environmental process on total diversity (Alroy et al., 2000; Badgley and Finarelli, 2013; Badgley et al., 2017; Blois and Hadly, 2009; Eronen et al., 2015; 92 Fraser et al., 2015; Janis, 1993; Janis and Wilhelm, 1993). Each of these studies provide a limited perspective on the macroevolutionary and macroecological processes shaping diversity and 94 diversification. Integration across perspectives is necessary for producing a holistic and internally consistent picture of how the North American mammal species pool has changed through time. One 96 of the goals of this study is to present a framework for approaching hypotheses about diversity and diversification through multiple lenses simultaneously through a joint model so that any inferences 98 are better constrained and the relative importance of species' ecological function, taxonomic affinities, and environmental context may be better elucidated.

100 The narrative of the diversification of North American mammals over the Cenozoic is one of gradual change. There is little convincing evidence that there have been any sudden 102 cross-functional or cross-taxonomic group turnover events in mammal diversity at any point in the Cenozoic record of North America (Alroy, 1996, 2009; Alroy et al., 2000; Eronen et al., 2015; Janis, 104 1993). Instead of being concentrated at specific time intervals, species turnover has been found to be distributed through time. It is then expected then that, for this analysis, turnover events or 106 periods of rapid diversification or depletion should not occur simultaneously for all functional groups under study. Additionally, changes to mammal diversification seem to be primarily driven by 108 changes to origination rate and not to extinction (Alroy, 1996, 2009; Alroy et al., 2000). An unresolved aspect of the general history of mammal diversification is whether that diversity is 110 limited or self-regulating; namely, to what extent is mammal diversification diversity-dependent

(Alroy, 2009; Harmon and Harrison, 2015; Rabosky, 2013; Rabosky and Hurlbert, 2015). Similarity,
112 this question can also be asked of specific functional groups (Jernvall and Fortelius, 2004; Quental
and Marshall, 2013; Silvestro et al., 2015; Van Valkenburgh, 1999).

114 Within the overall narrative of mammal diversity, the histories of some functional and taxonomic
groups are better understood than others. These groups include ungulate herbivores and Neogene
116 carnivores which have particularly good fossil records and have been the focus of previous analyses.

The diversity history of ungulate herbivores has been characterized by more recently originating
118 taxa having longer legs, higher crowned teeth, and a shift from graze-dominated to
browse-dominated diets than their earlier originating counterparts (Cantalapiedra et al., 2017;
120 Fraser et al., 2015; Janis et al., 2004; Janis, 1993, 2008; Janis et al., 2000). The mechanisms which
drive this pattern are theorized to be some combination of tectonic activity driving environmental
122 change such as the drying of the western interior of North America due mountain building and
global temperature and environmental change such as the formation of polar icecaps (Badgley et al.,
124 2017; Blois and Hadly, 2009; Eronen et al., 2015; Janis, 2008).

In contrast, the origination of modern cursorial carnivore forms was not until later in the Cenozoic;
126 this is not to say that carnivore diversity only grew in the late Cenozoic, but that those forms were
late entrants (Janis and Wilhelm, 1993). Instead, the diversity history of carnivores is reflective of
128 density-dependence or some other form of self-regulation (Silvestro et al., 2015; Slater, 2015; Van
Valkenburgh, 1999). Specifically, it has been proposed that different canid clades have replaced each
130 other as the dominate members of their functional group within the species pool (Silvestro et al.,
2015; Van Valkenburgh, 1999). It is then expected that, for this analysis, the diversity of digitigrade
132 and plantigrade carnivores (i.e. the “carnivore” guild of Van Valkenburgh (1999)) should be
relatively constant for the Cenozoic or at least have plateaued by the Neogene.

134 In a relevant study, Smits (2015) found that functional traits such as a species dietary or locomotor
category structure differences in mammal extinction risk. In particular, arboreal taxa were found to
136 have a shorter duration on average than species from other locomotor categories (Smits, 2015). Two
possible scenarios that could yield this pattern were proposed: the extinction risk faced by arboreal

138 species is constant and high for the entire Cenozoic or the Paleogene and Neogene represent
139 different regimes and extinction risk increased in the Neogene, thus driving up the Cenozoic average
140 extinction risk. These two possible explanations have clear and testable predictions with respect to
141 the diversity history of arboreal taxa: 1) if arboreal taxa always have an elevated extinction risk
142 when compared to other taxa, then the diversity history of arboreal taxa is expected to be constant
143 with time, albeit possibly at low diversity; and 2) if the Paleogene and Neogene represent difference
144 selective regimes with the former being associated with lower extinction risk than the latter, then
145 the diversity history of arboreal taxa are expected to be present in the Paleogene but depleted or
146 absent from the species pool during the Neogene.

There is a lack of consensus as to the effect of species body size on mammal diversity and aspects of
148 the diversification processes, specifically extinction (Liow et al., 2008, 2009; Smits, 2015; Tomiya,
149 2013). Species body size is frequently framed as an important biological descriptor because of its
150 correlation with other important and relevant ecological traits such as metabolic rate and home
151 range size (Brown, 1995). It is also relatively easy to estimate for extinct species using proxy
152 measures and regression equations, as was done in this study (see below). However, body size is
153 normally analyzed without simultaneous reference to other relevant species traits (Huang et al.,
154 2017; Liow et al., 2008; Raia et al., 2012; Smith et al., 2004), but see (Smits, 2015); this combined
155 with the high amount of correlation between life history traits and body size limits process-based
156 inference, because the actual causal mechanisms underlying an observed pattern are obscured or
157 missing.

158 The climate history of the Cenozoic can be broadly described as a gradual cooling trend, with polar
159 ice-caps forming in the Neogene (Cramer et al., 2011; Zachos et al., 2008, 2001). There are of course
160 exceptions to this pattern such as the Eocene climatic optimum, the mid-Miocene climatic
161 optimum, and the sudden drop in temperature at the Eocene/Oligocene boundary (Zachos et al.,
162 2008, 2001). In terms of the North American biotic environment, the Cenozoic is additionally
163 characterized by major transition from having closed, partially forested biomes being common in
164 the Paleogene to the landscape being dominated by savannah and grasslands biomes by the
Neogene (Blois and Hadly, 2009; Janis, 1993; Janis et al., 2000; Strömberg, 2005). Additionally, the

¹⁶⁶ landscape structure and topology of North America changed substantially over the Cenozoic with
¹⁶⁷ mountain uplift and other tectonic actives in Western North America (Badgley and Finarelli, 2013;
¹⁶⁸ Blois and Hadly, 2009; Eronen et al., 2015; Janis, 2008). This type of geological activity affects
¹⁶⁹ both local climates as well as continental weather patterns while also mobilizing increased grit into
¹⁷⁰ the environment, something which may be responsible for increasing trend of hyposodony (high
¹⁷¹ crowned teeth) among ungulate and rodent herbivores (Damuth and Janis, 2011; Janis, 1993;
¹⁷² Jardine et al., 2012; Jernvall and Fortelius, 2002) Badgley CITATION.

The Eocene-Oligocene transition has been observed to be associated with extinction of many
¹⁷⁴ ungulate taxa (Janis, 2008). This boundary also marks the transition from the Paleogene to the
Neogene and from herbivores being browsing dominated to grazing dominated, though not
¹⁷⁶ concurrently (Janis, 1993; Strömberg, 2005). Additionally, the Paleogene-Neogene boundary marks
the approximate start of Antarctic ice sheets, which were previously absent (Zachos et al., 2008).
¹⁷⁸ There is an observed stability in estimates of global temperature from the E/O transition till the
end of the Miocene called the Mid-Miocene climatic optimum (Zachos et al., 2008, 2001). The
¹⁸⁰ Mid-Miocene climatic optimum is bookended by periods of temperature decline. We would then
expect that, for the Miocene, turnover and other diversification events would most likely be due to
¹⁸² biological interactions or immigration and not biotic-abiotic interactions because of the constancy
of the climate, and that those groups that are driven primarily by environmental factors, the
¹⁸⁴ Miocene would be a period of marked by an absence of major changes to diversity or the
diversification process.

¹⁸⁶ The effect of climate on mammal diversity and its accompanying diversification process has been
the focus of considerable research with a slight consensus favoring mammal diversification being
¹⁸⁸ more biologically-mediated than climate-mediated when considering the entire Cenozoic (Alroy
et al., 2000; Clyde and Gingerich, 1998; Figueirido et al., 2012). However, differences in temporal
¹⁹⁰ and geographic scale seem to underly the contrast between these two perspectives. For example
when the mammal fossil record analyzed at small temporal and geographic scales a correlation
¹⁹² between diversity and climate is observable (Clyde and Gingerich, 1998). However, when the record
is analyzed at the scale of the continent and most of the Cenozoic this correlation disappears (Alroy

¹⁹⁴ et al., 2000). This result, however, does not go against the idea that there may be short periods of correlation between diversity and climate and that this relationship can change or even reverse
¹⁹⁶ direction over time; this type result means that there is no single direction or longterm correlation between diversity and climate (Figueirido et al., 2012).

¹⁹⁸ In the case of a fluctuating correlation between diversity and climate it is hard to make the argument for an actual causal link between the two without modeling the underlying ecological
²⁰⁰ differences between species; after all, species respond differently based on their individual ecologies (Blois and Hadly, 2009). When analysis is based on diversity or taxonomy alone no mechanisms are
²⁰² possible to infer. Taxonomy, like body size, stands in for many important species traits to the point that mechanistic or process based inference is impossible. While emergent patterns might
²⁰⁴ correspond to taxonomic grouping, this itself is an emergent phenomenon. Instead, by framing hypotheses in terms of species traits and their environmental context, these emergent phenomena
²⁰⁶ can be observed and analyzed rather than assumed.

Foreground

²⁰⁸ The fourth-corner problem is conceptual and statistical framework to explaining the patterns of either species abundance or presence/absence in a community as a product of species traits,
²¹⁰ environmental factors, and the interaction between traits and environment (Brown et al., 2014; Jamil et al., 2013; Pollock et al., 2012; Warton et al., 2015); effectively uniting climate-based species
²¹² distribution modeling (SDMs) with trait-based community assembly models (CATS, MaxEnt). The fourth-corner problem is normally phrased in modern ecological studies as understanding how traits
²¹⁴ and environment interact to predict the occurrence of species at localities distributed across a region (Jamil et al., 2013; Pollock et al., 2012).

²¹⁶ This conceptual framework can be extended to include time when considering occurrence as a three-dimensional: species at localities in space over time. This extension changes the goal of
²¹⁸ predicting just occurrence to one of predicting species gain and loss at localities. However, the temporal limitations of modern ecological studies limit studying species over their entire durations,

220 where speciation and extinction govern the occurrence of species. By considering the patterns of
fossil occurrences in the geological record the macroevolutionary processes governing species'
222 (macro)ecology can be better understood. One limitation of the fossil record, however, is a lack of
spatial resolution for most taxonomic groups and periods of time. As such, paleontological data
224 "looks" at a different side of the three-dimensional occurrence matrix of the extended fourth-corner
problem than modern ecological data.

226 In this study, the fourth-corner problem is phrased as understanding how mammal functional
groups respond to environmental change in order to predict the origination and survival of species
228 over time (Fig. 1). Additionally, I also consider the incompleteness of the fossil record and the static
effect of other species descriptors not related to functional group on origination and survival.

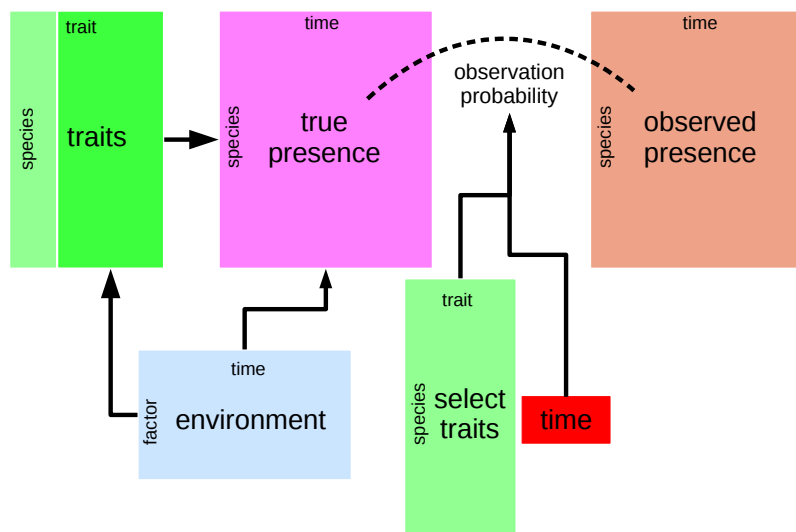


Figure 1: Conceptual diagram of the analysis at the center of this study. The observed presence matrix (orange) is the empirical presence/absence pattern for all species for all time points; this matrix is an incomplete observation of the "true" presence/absence pattern (purple). This observation process is modeled as a function of both time (red) and a selection of species traits (green). The estimated true presence matrix is modeled as a function of both environmental factors over time (blue) and multiple species traits (green). Additionally, the effects of environmental factors on some of those species traits are also modeled, as traits are expected to mediate the effects of a species environmental context. This diagram is based partially on material presented in Brown et al. (2014) and Warton et al. (2015).

230 My approach to delimiting and assigning mammal functional groups is inspired on the ecocube
heuristic used to classify marine invertebrate species by three functional traits (Bambach et al.,
232 2007; Bush and Bambach, 2011; Bush et al., 2007; Bush and Novack-Gottshall, 2012;
Novack-Gottshall, 2007; Villéger et al., 2011). In this study, the two functional traits used to define
234 a species' functional group are dietary (e.g. herbivore, carnivore, etc.) and locomotor category (e.g.
arboreal, unguligrade, etc.). Species body mass was also included as a species trait in this analysis,
236 but not as a trait for defining a functional group; instead, its inclusion is principally to control for
differences in species dynamics that driven by mass and not functional group.

238 The environmental covariates included in this study are estimates of global temperature as well as
which of three high-level North American plant taxonomic phases corresponds to that temporal
240 unit (Cramer et al., 2011; Graham, 2011). These covariates were chosen because they provide a
characterizations of the environmental context of the entire North American regional species pool
242 for most of the Cenozoic. Importantly, the effects of a species functional group on diversity are
themselves modeled as functions of environmental factors (Fig. 1) allowing for inference as to how a
244 species ecology can mediate selective pressures do to its environmental context.

All observations, paleontological or modern, are made with uncertainty. With presence/absence
246 data this uncertainty comes from not knowing if an absence is a “true” absence or just a failure to
observe (Foote, 2001; Foote and Sepkoski, 1999; Lloyd et al., 2011; Royle and Dorazio, 2008; Royle
248 et al., 2005; Wang and Marshall, 2016). For paleontological data, the incomplete preservation and
sampling of species means that the true times of origination or extinction may not be observed
250 (Foote, 2001; Foote and Sepkoski, 1999; Wang et al., 2016; Wang and Marshall, 2016). The model
used in this analysis is a translation of the conceptual framework described above (Fig. 1) into a
252 statistical model in order to estimate the relative diversity of mammal functional groups over time
and how those functional groups respond to changes to environmental context while taking into
254 account the fundamental incompleteness of the fossil record.

Ultimately, the goals of this analysis are to understand when are different functional groups
256 enriched or depleted in the North American mammal regional species pool and how these changes

in functional diversity are related to changes in species' environmental context. In the analysis
258 performed here, I consider multiple covariates which describe a species' macroecology and
environmental context. In order to analyze this complex, multi-level question and accompanying
260 highly-structured data set, I developed a hierachal Bayesian model combing the fourth-corner
modeling approach with a model of an observation-occurrence or observation-originatation-extinction
262 process.

Materials and Methods

264 Taxon occurrences and species-level information

All fossil occurrence information used in this analysis was downloaded from the Paleobiology
266 Database (PBDB). The initial download restricted occurrences to Mammalia observed in North
America between the Maastrichtian (72-66 Mya) and Gelasian (2.58-1.8 Mya) stages (Cohen et al.,
268 2015). Taxonomic, stratigraphic, and ecological metadata for each occurrence and species was also
downloaded. A new download for a raw, unfiltered PBDB datafile following the same criterion used
270 here is available at <http://goo.gl/2s1geU>. The raw datafile used as a part of this study, along
with all code for filtering and manipulating this download is available at
272 <http://github.com/psmits/copings>.

After being downloaded, the raw occurrence data was then sorted, cleaned, and manipulated
274 programmatically before analysis. Occurrences were restricted to those occurring between 64 and 2
million years ago (Mya); this age restriction was to insure that observation time series lines up with
276 the temperature time series (Cramer et al., 2011). All taxa whose life habit was classified as either
volant (i.e. Chiroptera) or aquatic (e.g. Cetacea) were excluded from this analysis because of their
278 lack of direct applicability to the study of terrestrial species pools.

Many species taxonomic assignments as present in the raw PBDB data were updated for accuracy
280 and consistency. Species present in the PBDB have some taxonomic information, including possible
Family and Order assignments. In order to increase consistency between species and reflect more

recent taxonomic assignments, each species taxonomic assignments updated as follows: 1) species family and order assignemnts as present in the Encyclopedia of life (<http://eol.org>) was downloaded using the *taxize* package for R; 2) for species not present in the EoL or not assigned order, their taxonomic inforation was further updated based on whatever family information was recorded in the PBDB or EoL; 3) for species still missing order assignemnts, their genus information was used to assign either an order or family, which was then used to assign an order.

This procedure is similar to that used in Smits (2015) and is detailed in the code repository associated with this study.

Species functional group is defined as the combination of locomotor and diet categories; the goal is to classify species based on the manner with which they interact with their environment. Mammal species records in the PBDB have life habit (i.e. locomotor category) and dietary category assignments. In order to simplify interpretation, analysis, and per-functional group sample size these classifications were coarsened in a similar manner to Smits (2015) (Table 1). Ground dwelling species locomotor categories were then reassigned based on the ankle posture associated with their taxonomic group, as described in Table 2 (Carrano, 1999). Ankle posture was assumed uniform for all species within a taxonomic group except for those species assigned a non-ground dwelling locomotor category in the PBDB, which retained their non-ground dwelling assignment. All species for which it was possible to assign a locomotor category had one assigned, including species for which post-cranaia are unknown but for which a taxonomic grouping is known. Ground dwelling species which were unable to be reassigned based on ankle posture were excluded from analysis.

Finally, ecotype categories with less than 10 total species were excluded, yielding a total of 18 observed ecotypes out of a possible 24.

Table 2: Ankle posture assignment as based on taxonomy. Assignments are based on (Carrano, 1999). Taxonomic groups are presented alphabetically and without reference for their relatedness.

Family	Stance
Ailuridae	plantigrade
Allomyidae	plantigrade

Continued on next page

Table 2 – continued from previous page

Family	Stance
Amphicyonidae	plantigrade
Amphilemuridae	plantigrade
Anthracotheriidae	digitigrade
Antilocapridae	unguligrade
Apheliscidae	plantigrade
Aplodontidae	plantigrade
Apternodontidae	scansorial
Arctocyonidae	unguligrade
Barbourofelidae	digitigrade
Barylambdidae	plantigrade
Bovidae	unguligrade
Camelidae	unguligrade
Canidae	digitigrade
Cervidae	unguligrade
Cimolodontidae	scansorial
Coryphodontidae	plantigrade
Cricetidae	plantigrade
Cylindrodontidae	plantigrade
Cyriacotheriidae	plantigrade
Dichobunidae	unguligrade
Dinocerata	unguligrade
Dipodidae	digitigrade
Elephantidae	digitigrade
Entelodontidae	unguligrade
Eomyidae	plantigrade

Continued on next page

Table 2 – continued from previous page

Family	Stance
Erethizontidae	plantigrade
Erinaceidae	plantigrade
Esthonychidae	plantigrade
Eutypomyidae	plantigrade
Felidae	digitigrade
Florentiamyidae	plantigrade
Gelocidae	unguligrade
Geolabididae	plantigrade
Glyptodontidae	plantigrade
Gomphotheriidae	unguligrade
Hapalodectidae	plantigrade
Heteromyidae	digitigrade
Hyaenidae	digitigrade
Hyaenodontidae	digitigrade
Hypertragulidae	unguligrade
Ischyromyidae	plantigrade
Jimomyidae	plantigrade
Lagomorpha	digitigrade
Leptictidae	plantigrade
Leptochoeridae	unguligrade
Leptomerycidae	unguligrade
Mammutidae	unguligrade
Megalonychidae	plantigrade
Megatheriidae	plantigrade
Mephitidae	plantigrade

Continued on next page

Table 2 – continued from previous page

Family	Stance
Merycoidodontidae	digitigrade
Mesonychia	unguligrade
Mesonychidae	digitigrade
Micropternodontidae	plantigrade
Mixodectidae	plantigrade
Moschidae	unguligrade
Muridae	plantigrade
Mustelidae	plantigrade
Mylagaulidae	fossorial
Mylodontidae	plantigrade
Nimravidae	digitigrade
Nothrotheriidae	plantigrade
Notoungulata	unguligrade
Oromerycidae	unguligrade
Oxyaenidae	digitigrade
Palaeomerycidae	unguligrade
Palaeoryctidae	plantigrade
Pampatheriidae	plantigrade
Pantolambdidae	plantigrade
Peritychidae	digitigrade
Perissodactyla	unguligrade
Phenacodontidae	unguligrade
Primates	plantigrade
Procyonidae	plantigrade
Proscalopidae	plantigrade

Continued on next page

Table 2 – continued from previous page

Family	Stance
Protoceratidae	unguligrade
Reithroparamyidae	plantigrade
Sciuravidae	plantigrade
Sciuridae	plantigrade
Simimyidae	plantigrade
Soricidae	plantigrade
Suidae	digitigrade
Talpidae	fossorial
Tayassuidae	unguligrade
Tenrecidae	plantigrade
Titanoideidae	plantigrade
Ursidae	plantigrade
Viverravidae	plantigrade
Zapodidae	plantigrade

304

Estimates of species mass used in this study were sourced from multiple databases and papers,
306 especially those focusing on similar macroevolutionary or macroecological questions (Brook and
Bowman, 2004; Freudenthal and Martín-Suárez, 2013; McKenna, 2011; Raia et al., 2012; Smith
308 et al., 2004; Tomiya, 2013); this is similar to Smits (2015). When a species' mass was not available,
proxy measures were used to estimate their mass. For example, given a measurement of a mammal
310 tooth size, it is possible and routine to estimate its mass given some regression equation. The
PBDB has one or more body part measures for many species. These were used as body size proxies
312 for many species, as was the case in Smits (2015). Mass was log-transformed and then rescaled by
first subtracting mean log-mass from all mass estimates, then dividing by two-times its standard
314 deviation; this insures that the magnitude of effects for both continuous and discrete covariates are

Table 1: Species trait assignments in this study are a coarser version of the information available in the PBDB. Information was coarsened to improve per category sample size.

This study		PBDB categories
Diet	Carnivore	Carnivore
	Herbivore	Browser, folivore, granivore, grazer, herbivore.
	Insectivore	Insectivore.
	Omnivore	Frugivore, omnivore.
Locomotor	Arboreal	Arboreal.
	Ground dwelling	Fossorial, ground dwelling, semifossorial, saltatorial.
	Scansorial	Scansorial.

directly comparable (Gelman, 2008; Gelman and Hill, 2007).

- 316 In total, 1400 mammal species occurrence histories were included in this study after applying all of
the restrictions above.

Table 3: Regression equations used in this study for estimating body size. Equations are presented with reference to taxonomic grouping, part name, and reference.

Group	Equation	log(Measurement)	Source
General	$\log(m) = 1.827x + 1.81$	lower m1 area	Legendre (1986)
General	$\log(m) = 2.9677x - 5.6712$	mandible length	Foster (2009)
General	$\log(m) = 3.68x - 3.83$	skull length	Luo et al. (2001)
Carnivores	$\log(m) = 2.97x + 1.681$	lower m1 length	Van Valkenburgh (1990)
Insectivores	$\log(m) = 1.628x + 1.726$	lower m1 area	Bloch et al. (1998)
Insectivores	$\log(m) = 1.714x + 0.886$	upper M1 area	Bloch et al. (1998)
Lagomorph	$\log(m) = 2.671x - 2.671$	lower toothrow area	Tomiya (2013)
Lagomorph	$\log(m) = 4.468x - 3.002$	lower m1 length	Tomiya (2013)
Marsupials	$\log(m) = 3.284x + 1.83$	upper M1 length	Gordon (2003)
Marsupials	$\log(m) = 1.733x + 1.571$	upper M1 area	Gordon (2003)
Rodentia	$\log(m) = 1.767x + 2.172$	lower m1 area	Legendre (1986)
Ungulates	$\log(m) = 1.516x + 3.757$	lower m1 area	Mendoza et al. (2006)
Ungulates	$\log(m) = 3.076x + 2.366$	lower m2 length	Mendoza et al. (2006)
Ungulates	$\log(m) = 1.518x + 2.792$	lower m2 area	Mendoza et al. (2006)
Ungulates	$\log(m) = 3.113x - 1.374$	lower toothrow length	Mendoza et al. (2006)

- 318 All fossil occurrences from 64 to 2 million years ago (Mya) were binned into the 19 North American
Land Mammal Ages (NALMA) covered by this interval CITATION. The choice of binning by
320 NALMA reflects the belief that these represent distinct communities or periods of mammal
evolution, something that is central to this study. Additionally, because of the inherently discrete
322 nature of the fossil record it can be hard to re-bin fossils by temporal interval because of the

Table 4: Definitions of the start and stop times of the three plant phases used this study as defined by Graham (2011).

Plant phase	Phase code	Start	Stop
Paleocene-Eocene	Pa-Eo	66	50
Eocene-Miocene	Eo-Mi	50	16
Miocene-Pleistocene	Mi-Pl	16	2

inherent uncertainty in their ages CITATION.

324 Environmental and temporal covariates

The environmental covariates used in this study are collectively referred to as group-level covariates
 326 because they predict the response of a “group” of individual-level observations (i.e. species
 occurrences of an ecotype). Additionally, these covariates are defined for temporal bins and not the
 328 species themselves; as such they predict the individual parts of each species occurrence history. The
 group-level covariates in this study are two global temperature estimates and the Cenozoic “plant
 330 phases” defined by Graham (2011).

Global temperature across most of the Cenozoic was calculated from Mg/Ca isotope record from
 332 deep sea carbonates (Cramer et al., 2011). Mg/Ca based temperature estimates are preferable to
 the frequently used $\delta^{18}\text{O}$ temperature proxy (Alroy et al., 2000; Figueirido et al., 2012; Zachos
 334 et al., 2008, 2001) because Mg/Ca estimates do not conflate temperature with ice sheet volume and
 depth/stratification changes. The former is particularly important to this analysis as the current
 336 polar ice-caps appeared and grew during the second half of the Cenozoic. These properties make
 Mg/Ca based temperature estimates preferable for macroevolutionary and macroecological studies
 338 (Ezard et al., 2016). Temperature was calculated as the mean of all respective estimates for each of
 the NALMA units. The distributions of temperature was then rescaled by subtracting its mean
 340 from all values and then dividing by twice its standard deviation.

The second set of environmental factors included in this study are the Cenozoic plant phases
 342 defined in Graham (2011). Graham’s plant phases are holistic descriptors of the taxonomic
 composition of 12 ecosystem types, which plants are present at a given time, and the relative

		State at $t + 1$		
		0_{never}	1	$0_{extinct}$
State at t	0_{never}	$1 - \pi$	π	0
	1	0	ϕ	$1 - \phi$
	$0_{extinct}$	0	0	1

Table 5: Transition matrix for the birth-death model (Eq. 1). Note that while there are only two state “codes” (0, 1), there are in fact three states: never having originated 0_{never} , present 1, extinct $0_{extinct}$ (Allen, 2011). The two modeled transition probabilities are origination π and survival ϕ .

344 modernity of those plant groups with younger phases representing increasingly modern taxa
 (Graham, 2011). Graham (2011) defines four intervals from the Cretaceous to the Pliocene, though
 346 only three of these intervals take place during the time frame being analyzed. Graham’s plant
 phases was included as a series of “dummy variables” encoding the three phases included in this
 348 analysis (Gelman and Hill, 2007); this means that the Miocene-Pleistocene phase is synonymous
 with the intercept and other phases are defined by their differences from this baseline. The
 350 temporal boundaries of these plant phases, their durations, and abbreviations are defined in Table 4.

Modelling species occurrence

352 At the core of the model used in this study is hidden Markov process where the latent process has
 an absorbing state; also refered to as a discrete-time birth-death model (Allen, 2011) or a
 354 capture-mark-recapture model CITATION. While there are only two state “codes” in a
 presence-absence matrix (i.e. 0/1), there are in fact three states in a birth-death model: not having
 356 originated yet, extant, and extinct. The last of these is the absorbing state, as once a species has
 gone extinct it cannot re-originate (Allen, 2011). Thus, in the transition matrices the probability of
 358 an extinct species changing states is 0 (Table 5). See below for parameter explanations (Tables 6, 7,
 and 8).

360 Basic model

I will begin defining the model used in this study by focusing on the basic machinery of the hidden
 362 Markov process at the model’s core. This basic model is similar to the Jolly-Seber

Table 6: Parameters associated with the hidden Markov Model at core of this model (Eq. 1). N is the number of species tracked in this study, and T is the number of time units (NALMAs) covered by this study.

Parameter	dimensions	explanation
y	$N \times T$	observed species presence/absence
z	$N \times T$	“true” species presence/absence
p	$N \times T$	probability of observing a species at time t if it is present
ϕ	$N \times T$	probability of species originating from time t to $t + 1$ if it is not present
π	$N \times (T - 1)$	probability of species surviving at time t , given that it is already originated

capture-mark-recapture model CITATION which has three characteristic probabilities: probability
364 p of observing a species given that it is present, probability π of a species surviving from one time
to another, and probability ϕ of a species first appearing (Royle and Dorazio, 2008) (Table 6). In
366 this formulation, the probability of a species becoming extinct is $1 - \pi$. The inclusion of species and
temporal information means that all three of these probabilities are defined for every species at
368 every time point (Table 6); how this is accomplished is described below. Importantly, only
origination can occur during the first time step as nothing is already present to survive.

$$\begin{aligned}
y_{i,t} &\sim \text{Bernoulli}(p_{i,t} z_{i,t}) \\
z_{i,1} &\sim \text{Bernoulli}(\phi_{i,1}) \\
z_{i,t} &\sim \text{Bernoulli} \left(z_{i,t-1} \pi_{i,t} + \sum_{x=1}^t (1 - z_{i,x}) \phi_{i,t} \right)
\end{aligned} \tag{1}$$

370 The parameters associated with Equation 1 are described in Table 6; this formulation is identical to
that described in Royle and Dorazio (2008). The product term that appears when calculating
372 values of z not at $t = 1$ ensures that once a species goes extinct it does not re-originate. The basic
model described here (Eq. 1) does not include the additional, necessary prior information which is
374 described below.

Expanding on the basics

376 Expanding on the basic model involves modeling the observation, origination and survival
probability as independent multi-level logistic regressions. Origination and survival probabilities

378 share the same covariates and model structure, but observation probability is modeled as a function
of a smaller selection of covariates.

380 The probability of observing a species given that it is present p is modeled as a logistic regression
with a time-varying intercept with an additional zero-centered varying effect for species' functional
382 group, respectively. The effect of species mass was also included through a slope term β^p .

The log-odds of a species originating (logit π) or surviving (logit ϕ) are modeled independently but
384 take the same form: a regression with an intercept that varies by both time and functional group,
an additional taxonomic order varying-intercept term, and the slope term for species mass.

386 Importantly, the time and functional group varying-intercept is itself modeled such that the
intercept for each functional group is a time series with group-level covariates (described below).

388 The expanded model incorporating these regression models is written as

$$\begin{aligned} y_{i,t} &\sim \text{Bernoulli}(p_{i,t} z_{i,t}) \\ p_{i,t} &= \text{logit}^{-1}(u_t + e_{j[i]} + \beta^p m_i) \\ z_{i,1} &\sim \text{Bernoulli}(\phi_{i,1}) \\ z_{i,t} &\sim \text{Bernoulli}\left(z_{i,t-1} \pi_{i,t} + \sum_{x=1}^t (1 - z_{i,x}) \phi_{i,t}\right) \\ \phi_{i,t} &= \text{logit}^{-1}(f_{j[i],t}^\phi + o_{k[i]}^\phi + \beta^\phi m_i). \\ \pi_{i,t} &= \text{logit}^{-1}(f_{j[i],t}^\pi + o_{k[i]}^\pi + \beta^\pi m_i) \end{aligned} \tag{2}$$

How the priors for the varying-effects and coefficients in this expanded model are described below
390 along with the complete model.

Complete model

392 The expanded model (Eq. 2) is still incomplete as it is missing the group-level covariates of interest
such as global temperature, and it is missing all of the necessary priors.

394 Here I describe how the effects of mammal functional group on origination and survival are

Table 7: Parameters for the first expansions

Parameter	dimensions	explanation
u	T	time-varying intercept
e	J	effect of functional group on observation
f^ϕ	$J \times T - 1$	intercept of log-odds ϕ , varies by time and functional group
f^π	$J \times T$	intercept of log-odds π , varies by time and functional group
o^ϕ	K	effect of species' order on log-odds of ϕ
o^π	K	effect of species' order on log-odds of π
β^ϕ	1	effect of species' mass on log-odds of ϕ
β^π	1	effect of species' mass on log-odds of π

modeled. f^ϕ and f^π are modeled as the responses from a multivariate normal distribution, where
 396 each functional group's time series is modeled as a regression. The time-series structure of these
 regressions is represented as a random-walk prior for the varying intercept of the group-level
 398 regressions. The effects of these group-level covariates on origination and survival are included for
 each functional group as a vector regression coefficients. The expansion to include this group-level
 400 regression is described in Equation 3, the parameters of which are described in Table 8.

$$\begin{aligned}
 f^\phi &\sim \text{MVN}(\mu^\phi, \Sigma^\phi) \\
 f^\pi &\sim \text{MVN}(\mu^\pi, \Sigma^\pi) \\
 \mu_{j,t}^\phi &= \alpha_{j,t}^\phi + U * \gamma_j^\phi \\
 \mu_{j,t}^\pi &= \alpha_{j,t}^\pi + U * \gamma_j^\pi \\
 \alpha_{j,t}^\phi &\sim \begin{cases} \mathcal{N}(0, 1) & \text{if } t = 1 \\ \mathcal{N}(\alpha_{j,t-1}^\phi, \sigma_j^\phi) & \text{if } t > 1 \end{cases} \\
 \alpha_{j,t}^\pi &\sim \begin{cases} \mathcal{N}(0, 1) & \text{if } t = 1 \\ \mathcal{N}(\alpha_{j,t-1}^\pi, \sigma_j^\pi) & \text{if } t > 1 \end{cases}
 \end{aligned} \tag{3}$$

In hierarchical models like the one described here (Eq. 2, 3) it can be hard to distinguish between
 402 the likelihood and prior as data can enter the model through many different parameters CITATION.
 For example, in Equation 2 the model of z can be considered a prior and statements in Equation 3

Table 8: Parameters for the group-level regressions. J is the number of functional groups, and D is the number of group-level covariates.

Parameter	dimensions	explanation
μ^ϕ	$J \times T$	time-series of the mean log-odds of ϕ for each functional group
μ^π	$J \times T$	time-series of the mean log-odds of π for each functional group
Σ^ϕ	$J \times J$	covariance matrix between functional groups for ϕ
Σ^π	$J \times J$	covariance matrix between functional groups for ϕ
α^ϕ	$J \times T$	time-varying intercept of μ^ϕ
α^π	$J \times T$	time-varying intercept of μ^π
σ^ϕ	J	scale of random-walk prior for α^ϕ
σ^π	J	scale of random-walk prior for α^π
γ^ϕ	D	group-level regression coefficients for μ^ϕ
γ^π	D	group-level regression coefficients for μ^π

404 can be considered priors for the parameters which predict ϕ and π . The remaining priors necessary
 to this model, however, are not based on parameter expansion but are prior estimates for the
 406 remaining unmodeled parameters and are sampling statements where no new data enters the model.
 These prior choices are expressed in Equation 4 and are explained below.

408 For the regression coefficients, such as β^ϕ and γ^ϕ , the chosen priors are considered weakly
 informative as they concentrate most of the probability density between -2 and 2. Similarly, the
 410 scale parameters, such as τ^ϕ and σ^ϕ , are also given weakly informative half-Normal priors which
 concentrate most of the probability density between 0 and -2. The covariance matrices, such as Σ^ϕ ,
 412 are decomposed into a vector of scale terms (e.g. τ^ϕ) and correlation matrices (e.g. Ω^ϕ) which were
 then given weakly informative priors. This approach and choice of LKJ priors for the correlation
 414 matrices follows the Stan User Manual CITATION. For parameter vectors which are presented with

only a single prior (e.g. β^ϕ), that prior statement is for each of the elements of that vector.

$$\begin{aligned}
e &\sim \mathcal{N}(0, \sigma^e) \\
\sigma^e &\sim \mathcal{N}^+(1) \\
\beta^p &\sim \mathcal{N}(0, 1) \\
o^\phi &\sim \mathcal{N}(0, v^\phi) \\
o^\pi &\sim \mathcal{N}(0, v^\pi) \\
v^\phi &\sim \mathcal{N}^+(1) \\
v^\pi &\sim \mathcal{N}^+(1) \\
\beta^\phi &\sim \mathcal{N}(0, 1) \\
\beta^\pi &\sim \mathcal{N}(0, 1) \\
\Sigma^\phi &= \text{diag}(\tau^\phi) \Omega^\phi \text{diag}(\tau^\phi) \\
\Sigma^\pi &= \text{diag}(\tau^\pi) \Omega^\pi \text{diag}(\tau^\pi) \\
\tau^\phi &\sim \mathcal{N}^+(1) \\
\tau^\pi &\sim \mathcal{N}^+(1) \\
\Omega^\phi &\sim \text{LKJ}(2) \\
\Omega^\pi &\sim \text{LKJ}(2) \\
\sigma^\phi &\sim \mathcal{N}^+(1) \\
\sigma^\pi &\sim \mathcal{N}^+(1) \\
\gamma^\phi &\sim \mathcal{N}(0, 1) \\
\gamma^\pi &\sim \mathcal{N}(0, 1)
\end{aligned} \tag{4}$$

- ⁴¹⁶ The model used in this study is the complete sampling statement expressed through the combination of equations 2, 3, and 4. These statements taken together form a complete generative
⁴¹⁸ model from which posterior inference of parameter values is possible.

Posterior inference and model adequacy

420 A computer program that implements joint posterior inference the model described above (Eqs. 2,
421 3, and 4) was written in the probabilistic programming language Stan (Stan Development Team,
422 2016). All methods for posterior inference implemented in Stan are derivative-based; this causes
complications for actually implementing the above models, because integers do not have derivatives.
424 In order to infer the values of the matrix of latent discrete parameters z (Tables 6) the log posterior
probabilities of all possible states of the unknown values of z were calculated and summed (i.e.
426 marginalized) (Stan Development Team, 2016).

Species durations at minimum range through from a species first appearance to their last
428 appearance in the fossil record, but the incompleteness of all observations means that the actual
times of origination and extinction are unknown. The marginalization approach used here means
430 that the (log) probabilities of all possible histories for a species are calculated, from the end
members of the species having existed for the entire study interval and the species having only
432 existed between the directly observed first and last appearances to all possible intermediaries (Fig
2) (Stan Development Team, 2016). Marginalization is identical, language-wise, to assuming
434 range-through and then estimating the (log) probability of all possible range extension due to
incomplete sampling.

436 The combined size of the dataset and large number of parameters (Eqs. 2, 3, and 4), in specific the
total number of latent parameters that are the matrix z , means that MCMC based posterior
438 inference is computationally slow. Instead, an approximate Bayesian approach was used: variational
inference. A recently developed automatic variational inference algorithm called “automatic
440 differentiation variational inference” (ADVI) is implemented in Stan and is used here (Kucukelbir
et al., 2015; Stan Development Team, 2016). ADVI assumes that the posterior is Gaussian but still
442 yields a true Bayesian posterior; this assumption is similar to quadratic approximation of the
likelihood function commonly used in maximum likelihood based inference (McElreath, 2016). The
444 principal limitation of assuming the joint posterior is Gaussian is that the true topology of the
log-posterior isn’t estimated; this is a particular burden for scale parameters which are bounded to

	Time Bin							
	1	2	3	4	5	6	7	8
Observed	0	0	0	1	0	1	1	0
-----	-----	-----	-----	-----	-----	-----	-----	-----
Certain	?	?	?	1	1	1	1	?
.....
Potential	0	0	0	1	1	1	1	0
Potential	0	0	1	1	1	1	1	0
Potential	0	1	1	1	1	1	1	0
Potential	1	1	1	1	1	1	1	0
Potential	0	0	0	1	1	1	1	1
Potential	0	0	1	1	1	1	1	1
Potential	0	1	1	1	1	1	1	1
Potential	1	1	1	1	1	1	1	1

Figure 2: Conceptual figure of all possible occurrence histories for an observed species. The first row represents the observed presence/absence pattern for a single species at eight time points. The second row corresponds to the known aspects of the “true” occurrence history of that species. The remaining rows correspond to all possible occurrence histories that are consistent with the observed data. By marginalizing over all possible occurrence histories, the probability of each potential history is estimated. The process of parameter marginalization is described in the text.

446 be positive (e.g. standard deviation).

Of additional concern for posterior inference is the partial identifiability of observation parameters
 448 $p_{t=1}$ and $p_{t=T}$ (Royle and Dorazio, 2008). This issue means that the estimates of sampling
 probabilities at the “edges” of the time series cannot fully be estimated because there are no known
 450 “gaps” in species occurrence histories that are guaranteed to be filled. Instead, the values of the first
 and final columns of the “true” presence-absence matrix z for those observations that do not already
 452 have presences in the observed presence-absence matrix y cannot be estimated (Royle and Dorazio,
 2008). The hierarchical modeling approach used here helps mitigate this problem by pulling the
 454 values of $p_{t=1}$ and $p_{t=T}$ towards the overall mean of p (Gelman et al., 2013), and in fact this
 approach might be more analytically sound than the more ad-hoc approaches that are occasionally
 456 used to overcome this hurdle (Royle and Dorazio, 2008). Additionally, because $p_{t=1}$ and $p_{t=T}$ are
 only partially identifiable, estimates of occurrence θ and origination ϕ at $t = 1$ and estimates of θ , ϕ

458 and survival π at $t = T$ may suffer from similar edge effects. Again, the hierarchical modeling
460 approach used here may help correct for this reality by drawing these estimates towards the overall
460 means of those parameters.

462 After obtaining approximate posterior inference using ADVI, model adequacy and quality of fit
464 were assessed using a posterior predictive check (Gelman et al., 2013). By simulating 100 theoretical
466 data sets from the posterior estimates of the model parameters and the observed covariate
468 information the congruence between predictions made by the model and the observed empirical
470 data can be assessed. These datasets are simulated by starting with the observed states of the
472 presence-absence matrix at $t = 1$; from there, the time series roll forward as stochastic processes
with covariate information given from the empirical observations. Importantly, this is fundamentally
different from observing the posterior estimates of the “true” presence-absence matrix z . The
posterior predictive check used in this study is to compare the observed average number of
observations per species to a distribution of simulated averages; if the empirically observed value
sits in the middle of the distribution then the model can be considered adequate in reproducing the
observed number of occurrences per species.

The ADVI assumption of a purely Gaussian posterior limits the utility and accuracy of the
474 posterior predictive checks because parameter estimates do not reflect the true posterior
distribution and are instead just an approximation (Gelman et al., 2013). Because of this, posterior
476 predictive estimates are themselves only approximate checks of model adequacy. The posterior
predictive check that is used in this study focuses on mean occurrence and not to any scale
478 parameters that might be most affected by the ADVI assumptions.

Given parameter estimates, diversity and diversification rates are estimated through posterior
480 predictive simulations. Given the observed presence-absence matrix y , estimates of the true
presence-absence matrix z can be simulated and the distribution of possible occurrence histories
482 can be analyzed. This is conceptually similar to marginalization where the probability of each
possible occurrence history is estimated (Fig. 2), but now these occurrence histories are generated
484 relative to their estimated probabilities.

The posterior distribution of z gives the estimate of standing diversity N_t^{stand} for all time points as

$$N_t^{stand} = \sum_{i=1}^M z_{i,t}. \quad (5)$$

- ⁴⁸⁶ Total regional standing diversity can also be partitioned into the standing diversity of each of the functional groups.

⁴⁸⁸ Results

The results of the analyses described above take one of two forms: direct inspection of posterior ⁴⁹⁰ parameter estimates, and downstream estimates of diversity and diversification rates based on posterior predictive simulations.

⁴⁹² Posterior parameter estimates

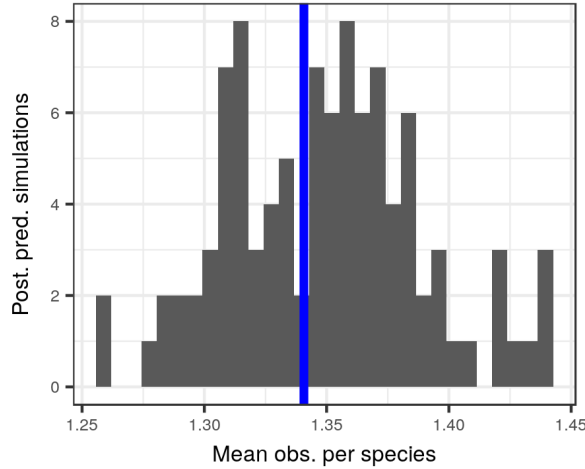


Figure 3: Comparison of the average observed number of occurrences per species (blue line) to the average number of occurrences from 100 posterior predictive datasets using the posterior estimates from the pure-presence and birth-death models.

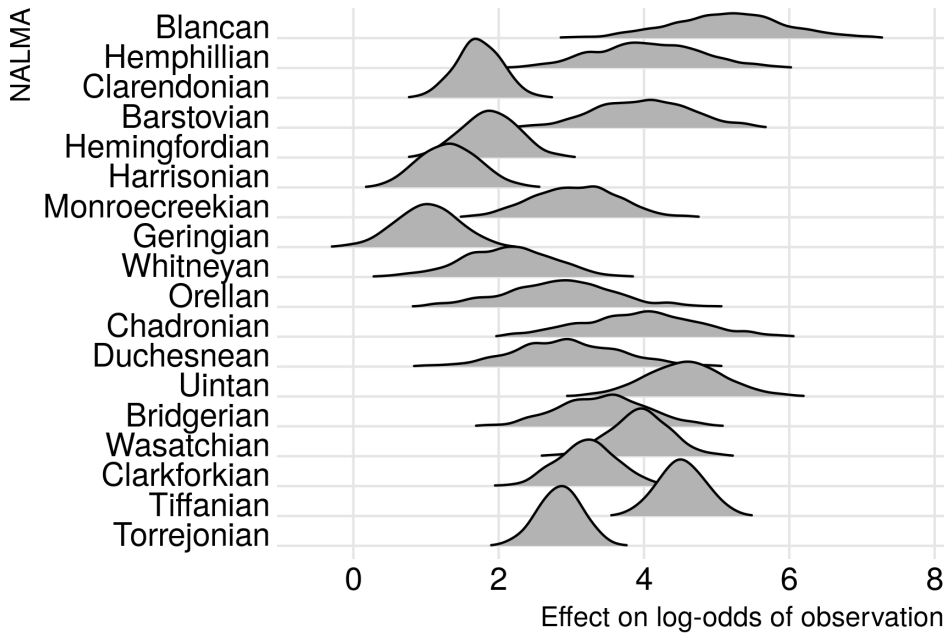


Figure 4

Analysis of diversity

- 494 All of the analyses of diversification and macroevolutionary rates has been done using only the birth-death model because of the model's better posterior predictive check performance (Fig. 3).
- 496 The general pattern of the estimated North American total mammal diversity for the Cenozoic is “stable” in that diversity fluctuates around a constant mean standing diversity, does not fluctuate 498 wildly and rapidly over the Cenozoic, and demonstrates no sustained directional trends (Fig. 13a). In broad strokes, the first 15 or so million years of the Cenozoic are characterized by first an 500 increase and then a decline in standing diversity at approximately 45-50 Mya (early-middle Eocene). Following this decline, standing diversity is broadly constant from 45 to 18 Mya (early Miocene).
- 502 After this, there is a rapid spike in diversity followed by a slight decline in diversity up to the Recent.
- 504 The pattern exhibited by the diversity history estimated in this study (Fig. 13a) has some major similarities with previous mammal diversity curves (Alroy, 2009): both curves begin with an 506 increase in diversity most of the major increases in diversity are retained including the large

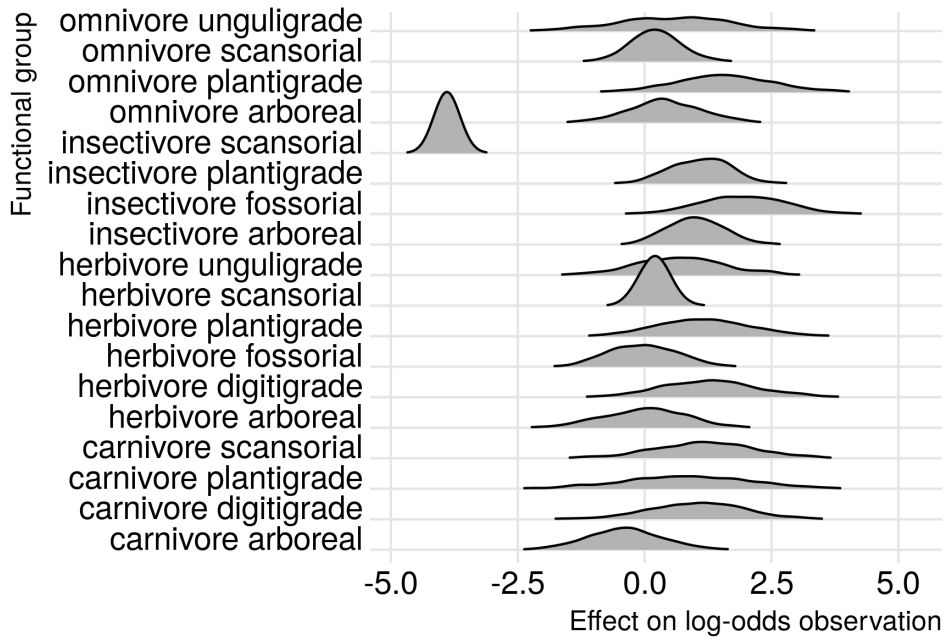


Figure 5

diversity spike during the Miocene. Unlike subsampling based approaches to estimating diversity

508 (Alroy, 2010), I'm able to interpolate over unsampled/poorly sampled time periods because of how
 the hierarchical model can share information across the different units Gelman et al. (2013); for
 510 cases like unsampled temporal bins, this may lead to estimates with high uncertainty, but that is
 preferable to no estimate at all. Finally, the Bayesian framework here gives a distribution of
 512 possible estimates of diversity allowing for direct inspection of the uncertainty of our inferences,
 something that is preferable to both traditional and resampling based confidence interval estimates
 514 (Gelman et al., 2013). Note that my time series of estimated diversity begins at a slightly different
 point than that of Alroy (2009) and that the time intervals used by Alroy (2009) are slightly shorter
 516 than those used here, so this may cause some of the minor differences between the curves. Also,
 please note that the diversity values are plotted at the “ceiling” of each temporal interval and not
 518 at the midpoint (Fig. 13a).

When viewed through the lens of diversification rate, some of the structure behind the estimated
 520 diversity history begins to take shape (Fig. 13b). For most of the Cenozoic, the diversification rate
 hovers around zero, punctuated by both positive and negative spikes. The largest spike in

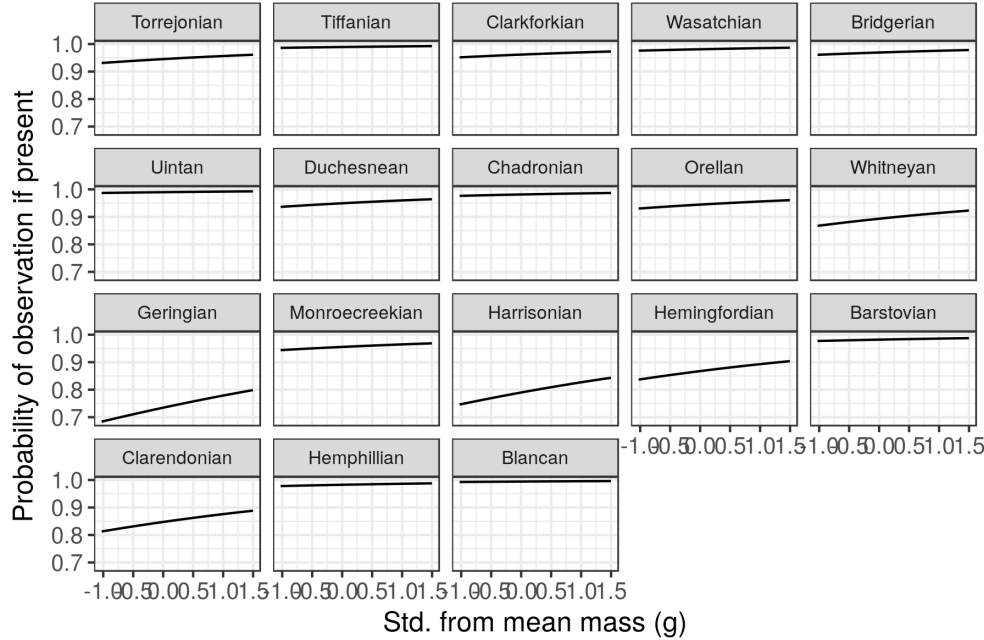


Figure 6: Estimates of the effect of species mass on probability of sampling a present species (p). Mass has been log-transformed, centered, and rescaled; this means that a mass of 0 corresponds to the mean of log-mass of all observed species and that mass is in standard deviation units. Estimates are from both the pure-presence and birth-death models.

- 522 diversification rate is at 16 Mya, which is early Oligocene (Fig. 13b). Other notable increases in
 diversification rate occur 56, 46, 22, 18, and 6 Mya (Table 13), though the last of these may be due
 524 to edge effects surrounding the partial-identifiability of $p_{t=T}$. Notable decreases in diversification
 rate occur at 54, 50, 48, 44, 40, 34, 30, 24, 20, 16, 12, and 8 Mya (Table 13), meaning that
 526 diversification rate has more major decreases than increases. While diversification rates significantly
 lower than average are more common than diversification rates greater than average, when
 528 diversification rate does increase it is with a greater magnitude than most decreases (Fig. 13b).
 Given that diversification rate more closely resembles origination rate than extinction rate (Fig.
 530 13b, 13c, 13d), these decreases in diversification rate may be indicative of “depletions” (failure to
 replace extinct taxa) rather than pulses of extinction.
- 532 The estimates from this study of per capita origination and extinction rates for the entire species
 pool (Fig. 13c, 13d) are very different from the origination and extinction rates estimated by Alroy
 534 (2009). The two most striking difference are the very different estimates of extinction rate between

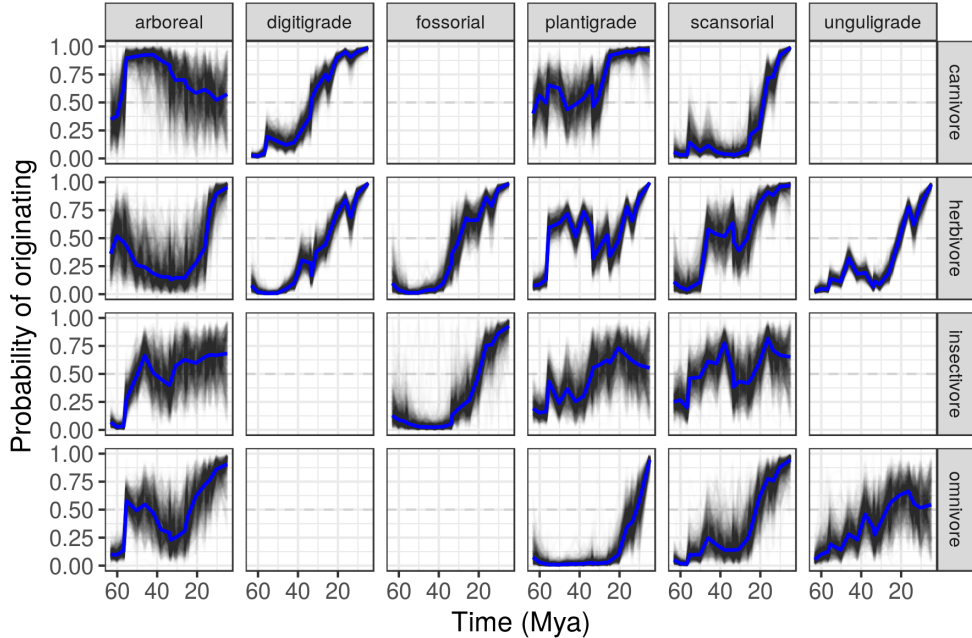


Figure 7: Probability of a mammal ecotype origination probabilities at each time point as estimated from the birth-death model. Each panel depicts 100 random samples from the model’s posterior. The columns are by locomotor category and rows by dietary category; their intersections are the observed and analyzed ecotypes. Panels with no lines are ecotypes not observed in the dataset.

the two studies and the very different scales of the origination rate estimates. This may be due to
 536 the fundamentally different way these rates are calculated, and how the diversification process was modeled. The per capita rates estimated in this study follow straight from the definition of a per
 538 capita rate (e.g. number of originations between time t and $t + 1$ divided by the diversity at time t) while the rates calculated in Alroy (2009) are based on log ratios of standing diversity.

540 The comparison between per capita origination and extinction rate estimates reveals how diversification rate is formed (Fig. 13c, 13d). As expected given previous inspection of the ecotype
 542 specific estimates of origination and survival probabilities from the birth-death model, diversification rate seems most driven by changes in origination rate as opposed to extinction rate.
 544 Extinction rate, on the other hand, demonstrates an almost saw-toothed pattern around a constant mean (Fig. 13d). These results are broadly consistent with those from previous analyses of North
 546 American mammals diversity and diversification (Alroy, 1996, 2009; Alroy et al., 2000).

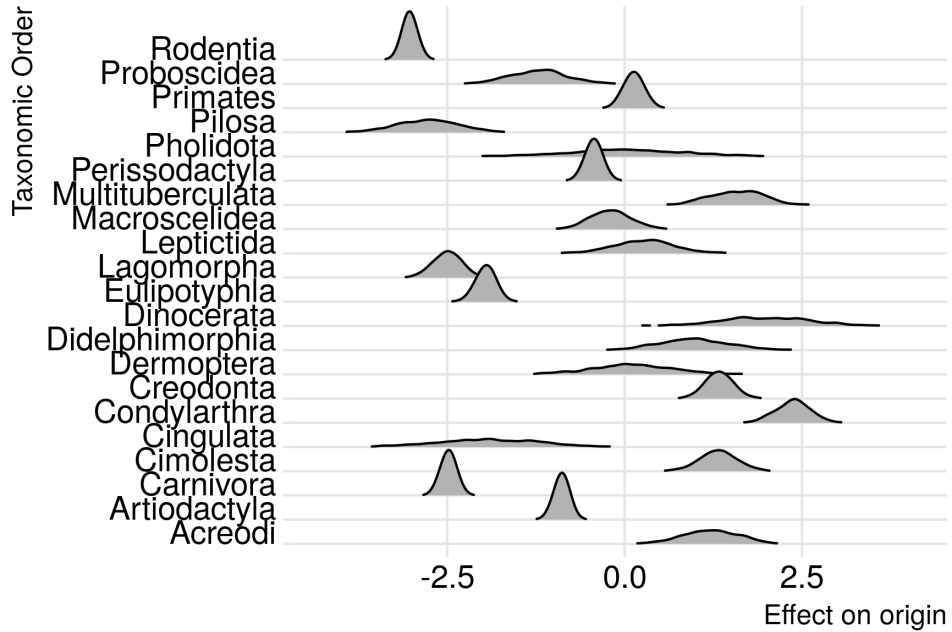


Figure 8

Diversity partitioned by ectype reveals a lot of the complexity behind the pattern of mammal

548 diversity for the Cenozoic (Fig. 14).

Arboreal ecotypes obtain peak diversity early in the Cenozoic and then decline for the rest of the
550 time series, becoming increasingly rare or absent as diversity approaches the Recent (Fig. 14).

Arboreal herbivores and omnivores obtain peak diversity at the beginning of the Cenozoic then go
552 into decline while remaining a small part of the species pool, while arboreal carnivores and
insectivores obtain peak diversity 52-50 Mya and then quickly decline and become extremely rare or
554 entirely absent from the species pool. This is consistent with increasing extinction risk in the
Neogene compared to the Paleogene as proposed by Smits (2015).

556 The diversity of digitigrade and unguligrade herbivores increases over the Cenozoic (Fig. 14). In
contrast, plantigrade herbivore diversity does not have a single, broad-strokes pattern; instead,
558 diversity increases, decreases, and may have then increased till the Recent. In contrast, fossorial and
scansorial herbivores demonstrate a much flatter history of diversity, with a slight increase in
560 diversity that over time is more pronounced among fossorial taxa than scansorial taxa. The

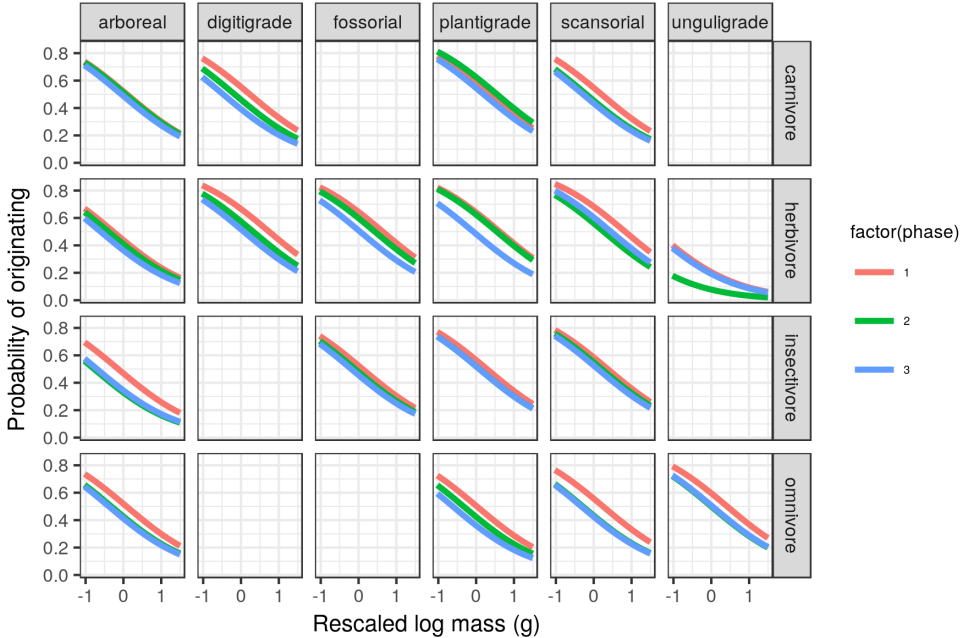


Figure 9: Mean estimate of the effect of species mass on the probability of a species originating for each of the three plant phases. The effect of mass is considered constant over time and that the only aspect of the model that changes with plant phase is the intercept of the relationship between mass and origination. The three plant phases are indicated by the color of the line. Mass has been log-transformed, centered, and rescaled; this means that a mass of 0 corresponds to the mean of log-mass of all observed species and that mass is in standard deviation units. For clarity, only the mean estimates of the effects of mass and plant phase are plotted.

expansion of digitigrade and unguiligrade herbivores over the Cenozoic is consistent with the

gradual expansion of grasslands which these ecotypes are better adapted to than closed environments (Blois and Hadly, 2009; Strömberg, 2005).

Digitigrade carnivores have a multi-modal diversity history, with peaks at 54-52 and 12-10 Mya (Fig.14). Between these two peaks digitigrade carnivore diversity dips below average diversity following the first peak and then grows slowly until the second peak. Plantigrade carnivores obtain peak diversity in the early Cenozoic and then maintain a relatively stable diversity until another peak at the end of the Cenozoic. The generally flat diversity history digitigrade carnivores lacks any sustained temporal trends and seems to reflect previous findings of limited diversity in spite of constant turnover and morphological evolution (Silvestro et al., 2015; Slater, 2015; Van Valkenburgh, 1999)

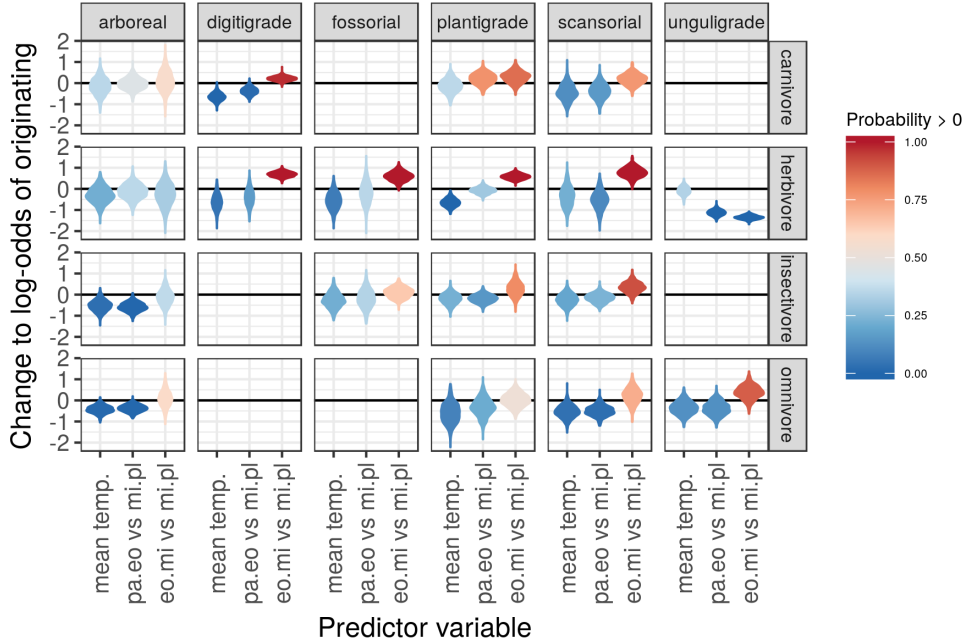


Figure 10: Estimated effects of the group-level covariates describing environmental context on log-odds of species origination. These estimates are from the birth-death model. What is plotted is a violin of the distribution of 1000 samples from the approximate posterior. The effect of plant phase graphed here is calculated as Phase 1= $\gamma_{phase\ 1}$, Phase 2= $\gamma_{phase\ 1} + \gamma_{phase\ 2}$, and so on.

- 572 There are some broad similarities in diversity histories of insectivorous and omnivorous taxa. The
 573 diversity histories of arboreal, plantigrade, and scansorial insectivorous taxa all demonstrate a
 574 decreasing pattern with time, while fossorial insectivores have a flat diversity history with a peak
 575 approximately 10 Mya (Fig. 14). Arboreal and scansorial omnivores decrease in diversity from their
 576 initial peaks early in the Cenozoic, and plantigrade omnivores have a generally flat diversity history
 577 with a sudden peak in diversity late in the Cenozoic (Fig. 14). Unguligrade omnivores also
 578 demonstrate a possible decrease in diversity over the Cenozoic, but not as clearly as arboreal and
 579 scansorial omnivores.
- 580 The waxing and waning of the mammal ecotypes is obvious when comparing changes to estimated
 581 relative log-mean of diversity (Fig. 15). While ecotype diversity does appear to change gradually,
 582 there are definite changes to the relative contributions of the ecotypes to the regional species pool.
 583 All arboreal ecotypes clearly decrease in relative diversity over the Cenozoic. In contrast the the
 584 digitigrade herbivore, fossorial herbivore, scansorial herbivore, and unculigrade herbivore ecotypes

Table 9: Posterior probability of the differences in the log-odds of an ecotype originating based on plant phase.

	P(Eo.Mi > 0)	P(Pa.Eo > 0)	P(Eo.Mi > Pa.Eo)
arboreal carnivore	0.575	0.447	0.598
digitigrade carnivore	0.976	0.017	0.998
plantigrade carnivore	0.857	0.780	0.578
scansorial carnivore	0.768	0.154	0.889
arboreal herbivore	0.318	0.357	0.428
digitigrade herbivore	1.000	0.161	0.995
fossorial herbivore	0.999	0.353	0.926
plantigrade herbivore	1.000	0.304	0.998
scansorial herbivore	0.999	0.108	0.998
unguligrade herbivore	0.000	0.000	0.100
arboreal insectivore	0.364	0.003	0.857
fossorial insectivore	0.645	0.341	0.708
plantigrade insectivore	0.794	0.148	0.881
scansorial insectivore	0.916	0.235	0.940
arboreal omnivore	0.590	0.006	0.882
plantigrade omnivore	0.524	0.209	0.762
scansorial omnivore	0.713	0.027	0.938
unguligrade omnivore	0.888	0.127	0.960

which increase in relative diversity over the Cenozoic. The digitigrade carnivore ecotype increases in
 586 relative diversity until approximately the start of the Neogene, after which it maintains a generally
 constant relative diversity; this is consistent with previous observations of constant or
 588 density-dependent diversity of the canid guild for the Neogene (Silvestro et al., 2015; Slater, 2015;
 Van Valkenburgh, 1999), a guild that overlaps with the digitigrade carnivore ecotype. Plantigrade
 590 herbivores remain a constant relative contribution to ecotypic diversity. These results support the
 hypothesis of a gradual transition from the early Paleogene with a region with more available
 592 habitat for arboreal taxa and less available habitat for many digitigrade and unguligrade taxa, to an
 environment where arboreal taxa are absent from the species pool and digitigrade and unguligrade
 594 taxa are much more dominant (Fig. 15). It is the relative contributions of digitigrade carnivores,
 digitigrade herbivores, and unguligrade herbivores which really shape the regional species pool of
 596 the Neogene.

Many of the estimated ecotype-specific diversity histories share a similar increase in diversity in the

Table 10: Posterior probability that the effects of the two temperature covariates on the log-odds of an ecotype origination are greater than 0. What is estimated is the probability that these estimates are greater than 0; high or low probabilities indicate the “strength” of the covariate in that direction (positive and negative, respectively). These estimates are from the birth-death model.

	$P(\gamma_{temp\ mean} > 0)$
arboreal carnivore	0.355
digitigrade carnivore	0.001
plantigrade carnivore	0.358
scansorial carnivore	0.121
arboreal herbivore	0.219
digitigrade herbivore	0.045
fossilorial herbivore	0.067
plantigrade herbivore	0.000
scansorial herbivore	0.221
unguligrade herbivore	0.339
arboreal insectivore	0.027
fossilorial insectivore	0.219
plantigrade insectivore	0.224
scansorial insectivore	0.192
arboreal omnivore	0.009
plantigrade omnivore	0.087
scansorial omnivore	0.035
unguligrade omnivore	0.129

598 late Cenozoic, 16-14 Mya (Fig. 14). These increases are either sustained or temporary and are seen
 in digitigrade carnivores, plantigrade carnivores, scansorial carnivores, unguiligrade herbivores,
 600 fossilorial insectivores, and plantigrade omnivores.

Discussion

602 Both the composition of a species pool and its environmental context change over time, though not necessarily at the same rate or concurrently. Local communities, whose species are drawn from the
 604 regional species pool, have “roles” in their communities defined by their interactions with a host of biotic and abiotic interactors (i.e. a species’ niche). For higher level ecological characterizations like
 606 ecotypes and guilds, these roles are broad and not defined by specific interactions but by the genre of interactions species within that grouping participate in. The diversity of species within an

Table 11: Posterior probability of the differences in the log-odds of an ecotype surviving based on plant phase.

	P(Eo.Mi > 0)	P(Pa.Eo > 0)	P(Eo.Mi > Pa.Eo)
arboreal carnivore	0.297	0.560	0.328
digitigrade carnivore	0.786	0.367	0.743
plantigrade carnivore	0.411	0.744	0.273
scansorial carnivore	0.428	0.445	0.486
arboreal herbivore	0.256	0.768	0.174
digitigrade herbivore	1.000	0.400	0.942
fossorial herbivore	0.696	0.563	0.565
plantigrade herbivore	0.659	0.508	0.596
scansorial herbivore	0.616	0.539	0.531
unguligrade herbivore	0.000	0.102	0.012
arboreal insectivore	0.289	0.483	0.368
fossorial insectivore	0.532	0.420	0.592
plantigrade insectivore	0.499	0.361	0.605
scansorial insectivore	0.443	0.252	0.634
arboreal omnivore	0.651	0.597	0.591
plantigrade omnivore	0.417	0.549	0.393
scansorial omnivore	0.486	0.525	0.487
unguligrade omnivore	0.929	0.521	0.844

608 ecotype or guild can be stable over millions of years despite constant species turnover (Jernvall and
 Fortelius, 2004; Slater, 2015; Van Valkenburgh, 1999). This implies that the size and scope of the
 610 role of an ecotype or guild in local communities, and the regional species pool as a whole, is
 preserved even as the individual interactors change. This also implies that the structure of regional
 612 species pools can be constant over time despite a constantly changing set of “players.” There is
 even evidence that functional groups are at least partially self-organizing and truly emergent
 614 (Scheffer and van Nes, 2006).

Comparison of the results from the posterior predictive checks for the pure-presence and birth-death
 616 models supports the conclusion that regional species pool dynamics cannot simply be described by
 a single occurrence probability and are instead the result of the interplay between the origination
 618 and extinction processes. Additionally, changes to the ecotypic composition and diversification rate
 of the North American regional species pool are driven primarily by variation in origination and not
 620 extinction (Fig. 13). These aspects of how regional species pool diversity is shaped are not directly

Table 12: Posterior probability that the effects of the two temperature covariates on the log-odds of an ecotype survival are greater than 0. What is estimated is the probability that these estimates are greater than 0; high or low probabilities indicate the “strength” of the covariate in that direction (positive and negative, respectively). These estimates are from the birth-death model.

	$P(\gamma_{temp\ mean} > 0)$
arboreal carnivore	0.665
digitigrade carnivore	0.453
plantigrade carnivore	0.618
scansorial carnivore	0.380
arboreal herbivore	0.761
digitigrade herbivore	0.395
fossorial herbivore	0.429
plantigrade herbivore	0.279
scansorial herbivore	0.345
unguligrade herbivore	0.818
arboreal insectivore	0.489
fossorial insectivore	0.452
plantigrade insectivore	0.435
scansorial insectivore	0.384
arboreal omnivore	0.600
plantigrade omnivore	0.639
scansorial omnivore	0.512
unguligrade omnivore	0.396

observable in studies of the Recent where time scales are short and macroevolutionary dynamics are

622 inferable solely from phylogeny (Fritz et al., 2013; Price and Schmitz, 2016).

Extinction rate for the entire regional species pool through time is highly variable and demonstrates

624 a saw-toothed pattern with no obvious temporal trends. While a constant mean extinction rate is consistent with previous observation (Alroy, 1996; Alroy et al., 2000), the degree to which mammal

626 extinction rate is actually variable may not have been equally appreciated as it has been for the marine invertebrate record (Foote, 2000a,b, 2006, 2010). What is most consistent with previous

628 observations, however, is that diversity seems to be most structured by changes to origination rather than changes to extinction (Alroy, 1996; Alroy et al., 2000).

630 Comparison of the ecotype specific diversity histories adds a considerable degree of nuance to broad narrative of shifts in functional composition of the North American mammal species pool as being
 632 gradual (Fig. 14). While most ecotypes do not experience sudden shifts in origination or extinction

Table 13: Posterior probabilities of diversity N_t^{stand} or diversification rate D_t^{rate} being greater than average standing diversity \bar{N}^{stand} or average diversification rate \bar{D}^{rate} for the whole Cenozoic. The “Time” column corresponds to the top of each of the temporal bins. Diversification rate can not be estimated for the last time point because it is unknown how many more species originated or went extinct following this temporal bin. The estimates are from the birth-death model.

NALMA	$P(N_t^{stand} > \bar{N}^{stand})$	$P(D_t^{rate} > \bar{D}^{rate})$
Torrejonian	0.79	
Tiffanian	0.95	0.67
Clarkforkian	0.50	0.03
Wasatchian	1.00	0.99
Bridgerian	0.69	0.00
Uintan	0.75	0.45
Duchesnean	0.00	0.00
Chadronian	0.01	0.70
Orellan	0.00	0.01
Whitneyan	0.00	0.09
Geringian	0.00	0.57
Monroecreekian	0.01	1.00
Harrisonian	0.11	0.67
Hemingfordian	0.96	0.99
Barstovian	1.00	1.00
Clarendonian	0.93	0.00
Hemphillian	0.63	0.10
Blancan	0.73	0.43

rate (Fig. 16, 17). As with the diversification rate of the entire species pool, the diversification of

individual ecotypes seem principally driven by origination and not extinction. Instead, while species seem to originate in waves (Fig. 16), they appear to leave the regional species pool in an

uncoordinated and individual manner (Fig. 17) which could be considered consistent with the maxim that all species respond differently to environmental change (Blois and Hadly, 2009). Note, however, this result characterizes the entire North American mammal regional species pool and thus may not reflect the dynamics of individual local communities.

The few large-magnitude, but temporary, increases in ecotype-specific origination rate occur in digitigrade carnivores, digitigrade herbivores, plantigrade herbivores, and unguligrade herbivores.

Importantly, the large peak in diversification and origination rates 16 Mya (Fig. 13) appears driven almost entirely by a massive increase in the origination rate of unguligrade herbivores (Fig. 16).

Additionally, there is some evidence that the origination probabilities of these ecotypes are

correlated (Fig. 11, ??). While this result does not mean that there are large and sudden
646 cross-ecotype changes to the regional species pool, it does suggest that additions to the species pool
do not occur in individual ecotypes idiosyncratically.

648 Arboreal taxa disappear from the regional species pool over the Cenozoic, with long term decline
over the Paleogene leading to the disappearance by start of Neogene ~22 Mya. This is partially
650 consistent with one of the two possible patterns presented here and in Smits (2015) that would
result in arboreal taxa having a greater extinction risk than other ecotypes: the Paleogene and
652 Neogene were different selective regimes and, while the earliest Cenozoic may have been neutral
with respect to arboreal taxa, they disappeared quickly over the Cenozoic which may account for
654 their higher extinction risk. However, these result add some nuance to this scenario as arboreal taxa
were declining throughout the Paleogene instead of maintaining a flat diversity as hypothesized
656 (Smits, 2015). I interpret the decline of arboreal taxa through out the Paleogene to mean that the
shift from closed to open environments began in the Paleogene and led to increasingly hostile
658 environments for arboreal taxa as opposed to being a sudden change in selective regime between
the Paleogene and Neogene. In addition to all arboreal taxa, the diversity of plantigrade and
660 scansorial insectivores decreases with time (Fig. 14).

Digitigrade carnivores have a relatively stable diversity history through the Cenozoic and can be
662 characterized as varying around a constant mean diversity. This ecotype has a large amount of
overlap with the carnivore guild which has been the focus of much research (Janis and Wilhelm,
664 1993; Pires et al., 2015; Slater, 2015; Van Valkenburgh, 1999). This result is consistent with some
form of “control” on the diversity of this ecotype, such as diversity-dependent diversification
666 (Silvestro et al., 2015; Slater, 2015; Van Valkenburgh, 1999).

Both digitigrade and unguligrade herbivores increase in diversity over the Cenozoic. The increase of
668 these cursorial forms is consistent with the gradual opening up of the North American landscape
(Blois and Hadly, 2009; Graham, 2011; Strömberg, 2005) and may indicate a long-term shift in the
670 interactors associated with those ecotypes leading to increased contribution to the regional species
pool. This result may be comparable to the increasing percentage of hypsodont (high-crowned

672 teeth) mammals in the Neogene of Europe being due to an enrichment of hyposodont taxa and not
a depletion of non-hypsodont taxa. Smaller scale increases in fossorial herbivore species, and a lesser
674 extent plantigrade herbivores, suggests that the increase of interactors may be associated mostly
with the herbivore dietary category with locomotor category tempering that relationship. These
676 results support the conclusion that the increase in digitigrade and unguligrade herbivores is the
result of an enrichment of these ecotypes as opposed to being caused by the depletion of other
678 herbivorous ecotypes; this is further supported by the lack of major changes to the number of
extinctions of all herbivore ecotypes (Fig. 17).

680 An association between plant phase and differences in ecotype occurrence or origination-extinction
probabilities is interpreted to mean that an ecotype enrichment or depletion is due to associations
682 between that ecotype and whatever plants are dominant at that time. Plant phase clearly
structures the occurrence and origination probability time series (Fig. ??, 4). These differences in
684 occurrence or origination translate to the estimates of diversity and diversification rate; the largest
spike in diversity, diversification rate, and origination rate all correspond to the onset of the last
686 plant phase (Fig. 13). The clearest example of the diversity of an ecotype increasing at this
particular transition is in scansorial carnivores (Fig. 14); similar shifts in other ecotypes are much
688 more subtle, as was previously noted for fossorial insectivores.

Interestingly, for all of the ecotypes with sudden changes in diversity at this transition the change is
690 an increase, even if only temporarily. There are two interpretations of these results. A biological
interpretation of this result is that, because plant phase associations are only with occurrence or
692 origination probabilities and not survival, these ecotypes were well suited for the newly available
mammal-plant interactions due to the increased modernization of their floral context (Graham,
694 2011). Alternatively, the increase in diversity associated with the third plant phase may be caused
by the edge effect in origination probability that is artificially inflating the number of origination
696 events (Fig. 4). However, the estimated number of origination events does not have a tremendous
spike at this transition, nor is a major increase in the number of origination events sustained (Fig.
698 16).

There are fewer, less obvious shifts in diversity surrounding the transition from the first to second
700 plant phase, with the following ecotypes having apparent shifts in diversity at 50 My: plantigrade
carnivores (down), arboreal omnivores (down), and scansorial omnivores (down). Arboreal
702 insectivore peak diversity also occurs 50 Mya, and is then followed by a steep decline in diversity
till 30 Mya when this ecotype is lost from the species pool. Because plant phase has been found to
704 structure occurrence/origination (Fig. ??, 4), but not survival (Fig. 5), my interpretation of these
results is that new species were not entering the system because there were fewer available
706 mammal-plant interactions available for those ecotypes. Instead, these ecotypes were poorly suited
for the newly available mammal-plant interactions brought upon by the changing environmental
708 context (Graham, 2011).

The temperature covariates are found to have similar effects on occurrence and origination
710 probabilities (Tables ??, 11). Temperature is found to more often affect ecotype occurrence
probabilities than origination probabilities. In most cases, there is a negative association between
712 temperature and probability of occurring or first originating; this means that if temperature
decreases, we would then expect an increase in the probability of occurring or first originating. In
714 contrast, temperature range is estimated to be a good predictor of survival in only to mammal
ecotypes and only marginally for one of those (Table 12). Additionally, both of these cases have
716 positive relationships, meaning that if temperature decreases it is expected that species survival will
also decrease.

718 The result that temperature does not affect the survival probability of most ecotypes is consistent
with previous analysis of mammal diversity (Alroy et al., 2000). The result that temperature affects
720 origination probability, on the other hand, is in strong contrast to the results Alroy et al. (2000).
An important difference between the analyses presented here and that of Alroy et al. (2000) is I am
722 considering the effect of temperature on the probability of a species originating, assuming it hasn't
originated yet while Alroy et al. (2000) analyzes the correlation between the first differences of the
724 origination and extinction rates with an oxygen isotope curve (Zachos et al., 2001). Origination or
extinction rates have very different properties than the origination probabilities estimated here
726 brought upon by the difference both in definition and units. Origination probability is the expected

probability that a species that has never been present and is not present at time t will be present at
728 time $t + 1$; origination probability is defined for a single species. In contrast, per capita rates are
defined (for origination) as the expected number of new species to have originated between time t
730 and $t + 1$ given the total number of species present at time t ; per capita rates are defined for the
standing diversity. It is also important to note that even though there is an edge effect at the last
732 time interval that causes an increase in the occurrence and origination probabilities of some
ecotypes (Fig. ??, 4, the corresponding rates and population level birth/death dynamics do not
734 share that pattern (Fig. 13, 16, 17). However, it is still possible that the finding that temperature
has an effect on origination may simply be because as time approaches the present the number of
736 species which have originated increases and not because of climatic forcing of origination.

All environmental factors are found to affect the occurrence and origination probabilities for most,
738 but not all, mammal ecotypes (Fig. ??, 9). In contrast, the environmental factors probably do not
affect differences in ecotype survival probability (Fig. 10). The focus in previous research on
740 temperature and major climatic or geological events without other measures of environmental
context may have led to confusion in discussions of how the “environment” affects mammal
742 diversity and diversification (Alroy et al., 2000; Figueirido et al., 2012). The environment or climate
are more than just global or regional temperature, it is also the set of all possible biotic and abiotic
744 interactions that can be experienced by a member of the species pool. By including more
descriptors of species’ environmental context than simple an estimate of global temperature a more
746 complete “picture” of the diversification process is inferred.

Analysis of relationship between temperature and origination rate is probably better suited for a
748 continuous-time birth-death or multilevel stochastic differential equation model instead of a
discrete-time model because the both continuous models estimate rates while discrete time models
750 estimate probabilities (Allen, 2011). The PyRate model(s) are based on a continuous-time
birth-death process (Silvestro et al., 2015, 2014). Unfortunately, a continuous-time model may be
752 unsuited for most paleontological data as the fossil record is naturally discrete; fossils are assigned
to temporal units, such as stages, which have age ranges. Individual fossils are not assigned
754 individual numeric ages. This reality was in fact my one of motivations for using discrete-time

birth-death model instead of one in continuous-time. There are of course exceptions to this
756 characterization; the fossil record of graptolites from the Ordovician and Silurian (Crampton et al.,
2016) and the fossil record of some mammal orders from Neogene are of high enough resolution that
758 the application of continuous-time models is appropriate and less fraught.

The effect of species mass on either occurrence or origination and extinction was not allowed to
760 vary by ecotype or environmental context. The primary reason for this modeling choice was that
this study focuses on ecotypic based differences in either occurrence, or origination and extinction.
762 Allowing the effect of body size to vary by ecotype, time, and environmental factors would increase
the overall complexity of the model beyond the scope of the study. Instead, body size was included
764 in order to control for its possible underlying effects (McElreath, 2016). A control means that if
there is variation due to body mass, having a term to “absorb” that effect is better than ignoring it.
766 The only covariate allowed to affect sampling probability was mass and only as a linear predictor.
Other covariates, such as the environmental factors considered here, could have affected the
768 underlying preservation process that limits sampling probability; their exclusion as covariates of
sampling/observation was the product of a few key decisions: model complexity, model
770 interpretability, the scope of this study, and a lack of good hypotheses related to these covariates to
warrant their inclusion.

772 Conclusions

These results add a considerable degree of nuance to the narrative of changes to North American
774 diversity being gradual. My results support the conclusions that ecotypic diversity is shaped more
by changes to origination than extinction and that major changes to total diversification rate can
776 be attributed to increases in origination of only some ecotypes. There are a number of interesting
estimated ecotype diversity patterns. While arboreal ecotypes are diverse in the Paleogene, by the
778 Neogene all arboreal ecotypes dramatically decreased in diversity and became either rare or absent
from the regional species pool. The other ecotypes that decrease in diversity over the Cenozoic are
780 plantigrade and scansorial insectivores and scansorial omnivores. The only ecotypes that

demonstrate a sustained pattern of increasing diversity are digitigrade and unguligrade herbivores.

782 When the environmental covariates analyzed here are inferred to affect the diversification of an
ecotype, this effect is virtually always on origination and not survival. This analysis provides a
784 much more complete picture of North American mammal diversity and diversification, specifically
the dynamics of the ecotypic composition of that diversity. By increasing the complexity of analysis
786 while precisely translating research questions into a statistical model, the context of the results is
much better understood. Future studies of diversity and diversification should incorporate as much
788 information as possible into their analyses in order to better understand or at least contextualize
the complex processes underlying that diversity.

790 Acknowledgements

I would like to thank K. Angielczyk, M. Foote, P. D. Polly, R. Ree, and G. Slater for helpful
792 discussion and advice. This entire study would not have been possible without the Herculean
effort of the many contributors to the Paleobiology Database. In particular, I would like to thank J.
794 Alroy and M. Uhen for curating most of the mammal occurrences recorded in the PBDB. This is
Paleobiology Database publication XXX.

796 References

- Allen, L. J. S. 2011. An introduction to stochastic processes with applications to biology. 2nd ed.
798 Chapman and Hall/CRC, Boca Raton, FL.
- Alroy, J. 1996. Constant extinction, constrained diversification, and uncoordinated stasis in North
800 American mammals. *Palaeogeography, Palaeoclimatology, Palaeoecology* 127:285–311.
- . 2009. Speciation and extinction in the fossil record of North American mammals. Pages
802 302–323 *in* R. K. Butlin, J. R. Bridle, and D. Schlüter, eds. *Speciation and patterns of diversity*.
Cambridge University Press, Cambridge.

- 804 ———. 2010. Fair sampling of taxonomic richness and unbiased estimation of origination and
extinction rates. Pages 55–80 *in* J. Alroy and G. Hunt, eds. Quantitative Methods in
806 Paleobiology. The Paleontological Society.
- Alroy, J., P. L. Koch, and J. C. Zachos. 2000. Global climate change and North American
808 mammalian evolution. *Paleobiology* 26:259–288.
- Badgley, C., and J. A. Finarelli. 2013. Diversity dynamics of mammals in relation to tectonic and
810 climatic history: comparison of three Neogene records from North America. *Paleobiology*
39:373–399.
- 812 Badgley, C., T. M. Smiley, R. Terry, E. B. Davis, L. R. G. Desantis, D. L. Fox, S. S. B. Hopkins,
T. Jezkova, M. D. Matocq, N. Matzke, J. L. McGuire, A. Mulch, B. R. Riddle, V. L. Roth, J. X.
814 Samuels, C. A. E. Strömberg, and B. J. Yanites. 2017. Biodiversity and Topographic Complexity:
Modern and Geohistorical Perspectives. *Trends in Ecology & Evolution* pages 1–16.
- 816 Bambach, R. K. 1977. Species richness in marine benthic habitats through the Phanerozoic.
Paleobiology 3:152–167.
- 818 Bambach, R. K., A. M. Bush, and D. H. Erwin. 2007. Autecology and the filling of ecospace: Key
metazoan radiations. *Palaeontology* 50:1–22.
- 820 Bloch, J. I., K. D. Rose, and P. D. Gingerich. 1998. New species of Batodonoides (Lipotyphla,
Geolabididae) from the Early Eocene of Wyoming: smallest known mammal? *Journal of
822 Mammalogy* 79:804–827.
- Blois, J. L., and E. A. Hadly. 2009. Mammalian Response to Cenozoic Climatic Change. *Annual
824 Review of Earth and Planetary Sciences* 37:181–208.
- Brook, B. W., and D. M. J. S. Bowman. 2004. The uncertain blitzkrieg of Pleistocene megafauna.
826 *Journal of Biogeography* 31:517–523.
- Brown, A. M., D. I. Warton, N. R. Andrew, M. Binns, G. Cassis, and H. Gibb. 2014. The

- 828 fourth-corner solution - using predictive models to understand how species traits interact with
the environment. *Methods in Ecology and Evolution* 5:344–352.
- 830 Brown, J. H., and B. A. Maurer. 1989. Macroecology: the division of food and space among species
on continents. *Science* 243:1145–1150.
- 832 Brown, J. J. 1995. *Macroecology*. University of Chicago Press, Chicago.
- Bush, A. M., and R. K. Bambach. 2011. Paleoeologic Megatrends in Marine Metazoa. *Annual
834 Review of Earth and Planetary Sciences* 39:241–269.
- Bush, A. M., R. K. Bambach, and G. M. Daley. 2007. Changes in theoretical ecospace utilization in
836 marine fossil assemblages between the mid-Paleozoic and late Cenozoic. *Paleobiology* 33:76–97.
- Bush, A. M., and P. M. Novack-Gottshall. 2012. Modelling the ecological-functional diversification
838 of marine Metazoa on geological time scales. *Biology Letters* 8:151–155.
- Cantalapiedra, J. L., J. L. Prado, and M. T. Alberdi. 2017. Decoupled ecomorphological evolution
840 and diversification in Neogene-Quaternary horses. *Science* 355:627–630.
- Carrano, M. T. 1999. What, if anything, is a cursor? Categories versus continua for determining
842 locomotor habit in mammals and dinosaurs. *Journal of Zoology* 247:29–42.
- Clyde, W. C., and P. D. Gingerich. 1998. Mammalian community response to the latest Paleocene
844 thermal maximum: an isotaphonomic study in the northern Bighorn Basin, Wyoming. *Geology*
26:1011–1014.
- 846 Cohen, K. M., S. C. Finney, P. L. Gibbard, and J.-X. Fan. 2015. The ICS International
Chronostratigraphic Chart.
- 848 Cottenie, K. 2005. Integrating environmental and spatial processes in ecological community
dynamics. *Ecology Letters* 8:1175–1182.
- 850 Cramer, B. S., K. Miller, P. Barrett, and J. Wright. 2011. Late Cretaceous-Neogene trends in deep
ocean temperature and continental ice volume: Reconciling records of benthic foraminiferal

- 852 geochemistry ($\delta^{18}\text{O}$ and Mg/Ca) with sea level history. *Journal of Geophysical Research: Oceans*
116:1–23.
- 854 Crampton, J. S., R. A. Cooper, P. M. Sadler, and M. Foote. 2016. Greenhouse-icehouse transition
in the Late Ordovician marks a step change in extinction regime in the marine plankton.
- 856 Proceedings of the National Academy of Sciences 113:1498–1503.
- 858 Damuth, J., and C. M. Janis. 2011. On the relationship between hypsodonty and feeding ecology in
ungulate mammals, and its utility in palaeoecology. *Biological Reviews* 86:733–758.
- 860 Elith, J., and J. R. Leathwick. 2009. Species distribution models: ecological explanation and
prediction across space and time. *Annual Review of Ecology, Evolution, and Systematics*
40:677–697.
- 862 Eronen, J. T., C. M. Janis, C. P. Chamberlain, and A. Mulch. 2015. Mountain uplift explains
differences in Palaeogene patterns of mammalian evolution and extinction between North
864 America and Europe. *Proceedings of the Royal Society B: Biological Sciences* 282:20150136.
- 866 Eronen, J. T., P. D. Polly, M. FRED, J. Damuth, D. C. FRANK, V. Mosbrugger,
C. SCHEIDEGGER, N. C. Stenseth, and M. Fortelius. 2010. Ecometrics: The traits that bind
the past and present together. *Integrative Zoology* 5:88–101.
- 868 Ezard, T. H. G., A. Purvis, and H. Morlon. 2016. Environmental changes define ecological limits to
species richness and reveal the mode of macroevolutionary competition. *Ecology Letters*
870 19:899–906.
- Felsenstein, J. 1985. Phylogenies and the comparative method. *The American Naturalist* 125:1–15.
- 872 Figueirido, B., C. M. Janis, J. A. Pérez-Claros, M. De Renzi, and P. Palmqvist. 2012. Cenozoic
climate change influences mammalian evolutionary dynamics. *Proceedings of the National
874 Academy of Sciences* 109:722–727.
- 876 Foote, M. 2000a. Origination and extinction components of taxonomic diversity: general problems.
Paleobiology 26:74–102.

- . 2000b. Origination and extinction components of taxonomic diversity: Paleozoic and
878 post-Paleozoic dynamics. *Paleobiology* 26:578–605.
- . 2001. Inferring temporal patterns of preservation, origination, and extinction from
880 taxonomic survivorship analysis. *Paleobiology* 27:602–630.
- . 2006. Substrate affinity and diversity dynamics of Paleozoic marine animals. *Paleobiology*
882 32:345–366.
- . 2010. The geologic history of biodiversity. Pages 479–510 in M. A. Bell, D. J. Futuyma,
884 W. F. Eanes, and J. S. Levinton, eds. *Evolution since Darwin: the first 150 years*. Sinauer
Associates, Sunderland, MA.
- 886 Foote, M., and J. J. Sepkoski. 1999. Absolute measures of the completeness of the fossil record.
Nature 398:415–7.
- 888 Foster, J. R. 2009. Preliminary body mass estimates for mammalian genera of the Morrison
Formation (Upper Jurassic, North America). *PaleoBios* 28:114–122.
- 890 Fraser, D., R. Gorelick, and N. Rybczynski. 2015. Macroevolution and climate change influence
phylogenetic community assembly of North American hoofed mammals. *Biological Journal of the
892 Linnean Society* 114:485–494.
- Freudenthal, M., and E. Martín-Suárez. 2013. Estimating body mass of fossil rodents. *Scripta
894 Geologica* 145:1–130.
- Fritz, S. A., J. Schnitzler, J. T. Eronen, C. Hof, K. Böhning-Gaese, and C. H. Graham. 2013.
896 Diversity in time and space: wanted dead and alive. *Trends in Ecology & Evolution* 28:509–16.
- Gelman, A. 2008. Scaling regression inputs by dividing by two standard deviations. *Statistics in
898 Medicine* pages 2865–2873.
- Gelman, A., J. B. Carlin, H. S. Stern, D. B. Dunson, A. Vehtari, and D. B. Rubin. 2013. Bayesian
900 data analysis. 3rd ed. Chapman and Hall, Boca Raton, FL.

- Gelman, A., and J. Hill. 2007. Data Analysis using Regression and Multilevel/Hierarchical Models.
902 Cambridge University Press, New York, NY.
- Gordon, C. L. 2003. A First Look at Estimating Body Size in Dentally Conservative Marsupials.
904 Journal of Mammalian Evolution page 21.
- Graham, A. 2011. A natural history of the New World: the ecology and evolution of plants in the
906 Americas. University of Chicago Press, Chicago.
- Harmon, L. J., and S. Harrison. 2015. Species Diversity Is Dynamic and Unbounded at Local and
908 Continental Scales. *The American Naturalist* 185:000–000.
- Harrison, S., and H. Cornell. 2008. Toward a better understanding of the regional causes of local
910 community richness. *Ecology Letters* 11:969–979.
- Huang, S., J. T. Eronen, C. M. Janis, J. J. Saarinen, D. Silvestro, and S. A. Fritz. 2017. Mammal
912 body size evolution in North America and Europe over 20 Myr: similar trends generated by
different processes. *Proceedings of the Royal Society B: Biological Sciences* 284:20162361.
- 914 Jamil, T., W. A. Ozinga, M. Kleyer, and C. J. F. Ter Braak. 2013. Selecting traits that explain
species-environment relationships: A generalized linear mixed model approach. *Journal of
916 Vegetation Science* 24:988–1000.
- Janis, C., J. Damuth, and J. M. Theodor. 2004. The species richness of Miocene browsers, and
918 implications for habitat type and primary productivity in the North American grassland biome.
Palaeogeography, Palaeoclimatology, Palaeoecology 207:371–398.
- 920 Janis, C. M. 1993. Tertiary mammal evolution in the context of changing climates, vegetation, and
tectonic events. *Annual Review of Ecology and Systematics* 24:467–500.
- 922 ———. 2008. An evolutionary history of browsing and grazing ungulates. Pages 21–45 *in* I. J.
Gordon and H. H. T. Prins, eds. *The Ecology of Browsing and Grazing*. Springer-Verlag.
- 924 Janis, C. M., J. Damuth, and J. M. Theodor. 2000. Miocene ungulates and terrestrial primary

- productivity: where have all the browsers gone? Proceedings of the National Academy of Sciences
926 97:7899–904.
- Janis, C. M., and P. B. Wilhelm. 1993. Were there mammalian pursuit predators in the tertiary?
928 Dances with wolf avatars. *Journal of Mammalian Evolution* 1:103–125.
- Jardine, P. E., C. M. Janis, S. Sahney, and M. J. Benton. 2012. Grit not grass: concordant patterns
930 of early origin of hypodonty in Great Plains ungulates and Glires. *Palaeogeography,
Palaeoclimatology, Palaeoecology* 365–366:1–10.
- 932 Jernvall, J., and M. Fortelius. 2002. Common mammals drive the evolutionary increase of
hypodonty in the Neogene. *Nature* 417:538–40.
- 934 ———. 2004. Maintenance of trophic structure in fossil mammal communities: site occupancy and
taxon resilience. *The American Naturalist* 164:614–624.
- 936 Kucukelbir, A., R. Ranganath, A. Gelman, and D. M. Blei. 2015. Automatic Variational Inference
in Stan. Pages 568–576 *in* NIPS. Vol. 28.
- 938 Legendre, S. 1986. Analysis of mammalian communities from the Late Eocene and Oligocene of
Southern France. *Paleovertebrata* 16:191–212.
- 940 Liow, L. H., M. Fortelius, E. Bingham, K. Lintulaakso, H. Mannila, L. Flynn, and N. C. Stenseth.
2008. Higher origination and extinction rates in larger mammals. *Proceedings of the National
942 Academy of Sciences* 105:6097–6102.
- Liow, L. H., M. Fortelius, K. Lintulaakso, H. Mannila, and N. C. Stenseth. 2009. Lower Extinction
944 Risk in SleeporHide Mammals. *The American Naturalist* 173:264–272.
- Lloyd, G. T., J. R. Young, and A. B. Smith. 2011. Taxonomic Structure of the Fossil Record is
946 Shaped by Sampling Bias. *Systematic Biology* 61:80–89.
- Loeuille, N., and M. a. Leibold. 2008. Evolution in metacommunities: on the relative importance of
948 species sorting and monopolization in structuring communities. *The American naturalist*
171:788–99.

- 950 Losos, J. B. 2010. Adaptive radiation, ecological opportunity, and evolutionary determinism. *The American naturalist* 175:623–39.
- 952 Losos, J. B., and D. L. Mahler. 2010. Adaptive radiation: the interaction of ecological opportunity, adaptation, and speciation. Chap. 15, pages 381–420 *in* M. A. Bell, D. J. Futuyma, W. F. Eanes, and J. S. Levinton, eds. *Evolution since Darwin: the first 150 years*. Sinauer Associates, Sunderland, MA.
- 954
- 956 Luo, Z.-X., A. W. Crompton, and A.-L. Sun. 2001. A New Mammaliaform from the Early Jurassic and Evolution of Mammalian Characteristics. *Science* 292:1535–1540.
- 958 McElreath, R. 2016. *Statistical rethinking: a Bayesian course with examples in R and Stan*. CRC Press, Boca Raton, FL.
- 960 McGill, B. J., B. J. Enquist, E. Weiher, and M. Westoby. 2006. Rebuilding community ecology from functional traits. *TRENDS in Ecology and Evolution* 21:178–185.
- 962 McKenna, R. T. 2011. Potential for Speciation in Mammals Following Vast , Late Miocene Volcanic Interruptions in the Pacific Northwest. Masters. Portland State University.
- 964 Mendoza, M., C. M. Janis, and P. Palmqvist. 2006. Estimating the body mass of extinct ungulates: a study on the use of multiple regression. *Journal of Zoology* 270:90–101.
- 966 Mittelbach, G. G., and D. W. Schemske. 2015. Ecological and evolutionary perspectives on community assembly. *Trends in Ecology and Evolution* 30:241–247.
- 968 Novack-Gottshall, P. M. 2007. Using a theoretical ecospace to quantify the ecological diversity of Paleozoic and modern marine biotas Using a theoretical ecospace to quantify the ecological diversity of Paleozoic and modern marine biotas. *Paleobiology* 33:273–294.
- 970
- 972 Pires, M. M., D. Silvestro, and T. B. Quental. 2015. Continental faunal exchange and the asymmetrical radiation of carnivores. *Proceedings of the Royal Society B: Biological Sciences* 282:20151952.

- 974 Pollock, L. J., W. K. Morris, and P. A. Vesk. 2012. The role of functional traits in species
distributions revealed through a hierarchical model. *Ecography* 35:716–725.
- 976 Polly, P., J. Eronen, M. Fred, G. P. Dietl, V. Mosbrugger, C. Scheidegger, D. C. Frank, J. Damuth,
N. C. Stenseth, and M. Fortelius. 2011. History matters: ecometrics and integrative climate
978 change biology. *Proceedings of the Royal Society B: Biological Sciences* 278:1131–1140.
- 980 Polly, P. D., A. M. Lawing, J. T. Eronen, and J. Schnitzler. 2015. Processes of ecometric patterning:
modelling functional traits, environments, and clade dynamics in deep time. *Biological Journal of
the Linnean Society* pages n/a–n/a.
- 982 Price, S. A., and L. Schmitz. 2016. A promising future for integrative biodiversity research: an
increased role of scale-dependency and functional biology. *Philosophical Transactions of the
984 Royal Society B: Biological Sciences* 371:20150228.
- 986 Quental, T. B., and C. R. Marshall. 2013. How the Red Queen Drives Terrestrial Mammals to
Extinction. *Science* 341:290–292.
- 988 Rabosky, D. L. 2013. Diversity-Dependence, Ecological Speciation, and the Role of Competition in
Macroevolution. *Annual Review of Ecology, Evolution, and Systematics* 44:1–22.
- 990 Rabosky, D. L., and A. H. Hurlbert. 2015. Species Richness at Continental Scales Is Dominated by
Ecological Limits. *The American Naturalist* 185:000–000.
- 992 Raia, P., F. Carotenuto, F. Passaro, D. Fulgione, and M. Fortelius. 2012. Ecological specialization
in fossil mammals explains Cope’s rule. *The American Naturalist* 179:328–37.
- 994 Royle, J. A., and R. M. Dorazio. 2008. Hierarchical modeling and inference in ecology: the analysis
of data from populations, metapopulations and communities. Elsevier, London.
- 996 Royle, J. A., J. D. Nichols, and M. Kéry. 2005. Modelling occurrence and abundance of species
when detection is imperfect. *Oikos* 110:353–359.
- 998 Scheffer, M., and E. H. van Nes. 2006. Self-organized similarity, the evolutionary emergence of
groups of similar species. *Proceedings of the National Academy of Sciences* 103:6230–6235.

- Shipley, B., D. Vile, and E. Garnier. 2006. From plant traits to plant communities: a statistical
1000 mechanistic approach to biodiversity. *Science* 314:812–814.
- Silvestro, D., A. Antonelli, N. Salamin, and T. B. Quental. 2015. The role of clade competition in
1002 the diversification of North American canids. *Proceedings of the National Academy of Sciences of
the United States of America* 112:8684–9.
- 1004 Silvestro, D., J. Schnitzler, L. H. Liow, A. Antonelli, and N. Salamin. 2014. Bayesian estimation of
speciation and extinction from incomplete fossil occurrence data. *Systematic biology* 63:349–67.
- 1006 Simberloff, D., and T. Dayan. 1991. The Guild Concept and the Structure of Ecological
Communities. *Annual Review of Ecology and Systematics* 22:115–143.
- 1008 Slater, G. J. 2015. Iterative adaptive radiations of fossil canids show no evidence for
diversity-dependent trait evolution. *Proceedings of the National Academy of Sciences*
1010 112:4897–4902.
- Smith, F. A., J. Brown, J. Haskell, and S. Lyons. 2004. Similarity of mammalian body size across
1012 the taxonomic hierarchy and across space and time. *The American Naturalist* 163:672–691.
- Smith, F. A., S. K. Lyons, S. Morgan Ernest, and J. H. Brown. 2008. Macroecology: more than the
1014 division of food and space among species on continents. *Progress in Physical Geography*
32:115–138.
- 1016 Smits, P. D. 2015. Expected time-invariant effects of biological traits on mammal species duration.
Proceedings of the National Academy of Sciences 112:13015–13020.
- 1018 Stan Development Team. 2016. Stan Modeling Language Users Guide and Reference Manual.
- Strömberg, C. A. E. 2005. Decoupled taxonomic radiation and ecological expansion of open-habitat
1020 grasses in the Cenozoic of North America. *Proceedings of the National Academy of Sciences of
the United States of America* 102:11980–4.
- 1022 Tomiya, S. 2013. Body Size and Extinction Risk in Terrestrial Mammals Above the Species Level.
The American Naturalist 182:196–214.

- 1024 Urban, M. C., M. A. Leibold, P. Amarasekare, L. De Meester, R. Gomulkiewicz, M. E. Hochberg,
C. A. Klausmeier, N. Loeuille, C. de Mazancourt, J. Norberg, J. H. Pantel, S. Y. Strauss,
1026 M. Vellend, and M. J. Wade. 2008. The evolutionary ecology of metacommunities. *Trends in
Ecology and Evolution* 23:311–317.
- 1028 Valentine, J. W. 1969. Patterns of taxonomic and ecological structure of the shelf benthos during
Phanerozoic time. *Paleontology* 12:684–709.
- 1030 Van Valkenburgh, B. 1990. Skeletal and dental predictors of body mass in carnivores. Pages
181–205 *in* J. Damuth and B. J. Macfadden, eds. *Body size in mammalian paleobiology:
estimation and biological implications*. Cambridge University Press, Cambridge.
- 1032 ———. 1999. Major patterns in the history of carnivorous mammals. *Annual Review of Earth and
Planetary Sciences* 27:463–493.
- 1034 Villéger, S., P. M. Novack-Gottshall, and D. Mouillot. 2011. The multidimensionality of the niche
reveals functional diversity changes in benthic marine biotas across geological time. *Ecology
Letters* 14:561–8.
- 1038 Wang, S. C., P. J. Everson, H. J. Zhou, D. Park, and D. J. Chudzicki. 2016. Adaptive credible
intervals on stratigraphic ranges when recovery potential is unknown. *Paleobiology* 42:240–256.
- 1040 Wang, S. C., and C. R. Marshall. 2016. Estimating times of extinction in the fossil record. *Biology
Letters* 12:20150989.
- 1042 Warton, D. I., B. Shipley, and T. Hastie. 2015. CATS regression - a model-based approach to
studying trait-based community assembly. *Methods in Ecology and Evolution* 6:389–398.
- 1044 Weber, M. G., C. E. Wagner, R. J. Best, L. J. Harmon, and B. Matthews. 2017. Evolution in a
Community Context: On Integrating Ecological Interactions and Macroevolution. *Trends in
Ecology & Evolution* xx:1–14.
- 1046 Wilson, J. B. 1999. Guilds, functional types and ecological groups. *Oikos* 86:507–522.
- 1048 Yoder, J. B., E. Clancey, S. Des Riches, J. M. Eastman, L. Gentry, W. Godsoe, T. J. Hagey,

- D. Jochimsen, B. P. Oswald, J. Robertson, B. A. J. Sarver, J. J. Schenk, S. F. Spear, and L. J.
1050 Harmon. 2010. Ecological opportunity and the origin of adaptive radiations. *Journal of
Evolutionary Biology* 23:1581–1596.
- 1052 Zachos, J. C., G. R. Dickens, and R. E. Zeebe. 2008. An early Cenozoic perspective on greenhouse
warming and carbon-cycle dynamics. *Nature* 451:279–283.
- 1054 Zachos, J. C., M. Pagani, L. Sloan, E. Thomas, and K. Billups. 2001. Trends, rhythms, and
aberrations in global climate 65 Ma to present. *Science* 292:686–693.

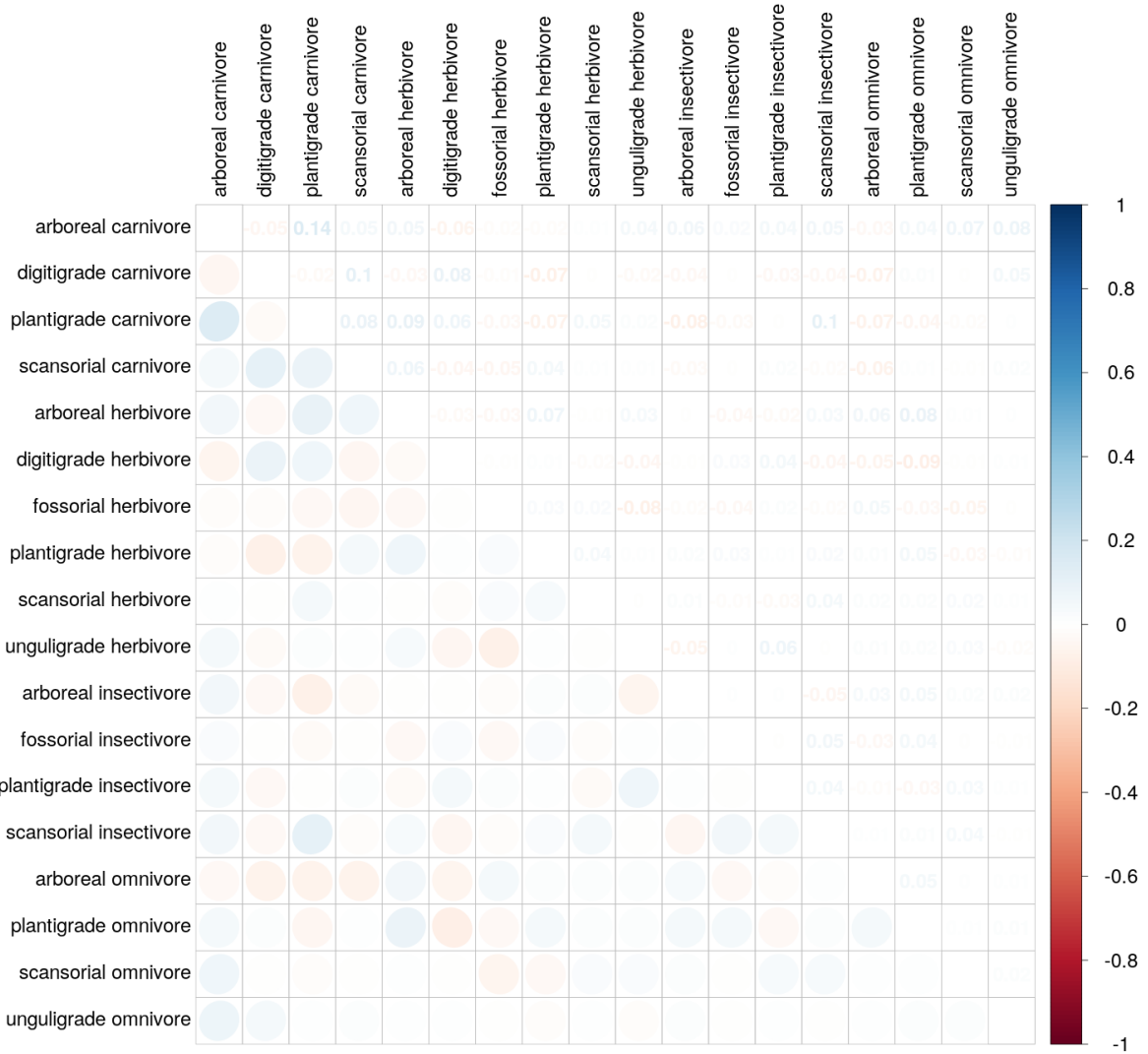


Figure 11: Posterior mean estimates of the correlations in origination probability between the mammal ecotypes. The lower triangle of the matrix is populated with ellipses corresponding to the level of correlation between the two ecotypes, while the upper triangle of the matrix corresponds to the mean estimated correlation between ecotypes. Darker values correspond to a greater magnitude of correlation with blue values corresponding to a positive correlation and red values a negative correlation.

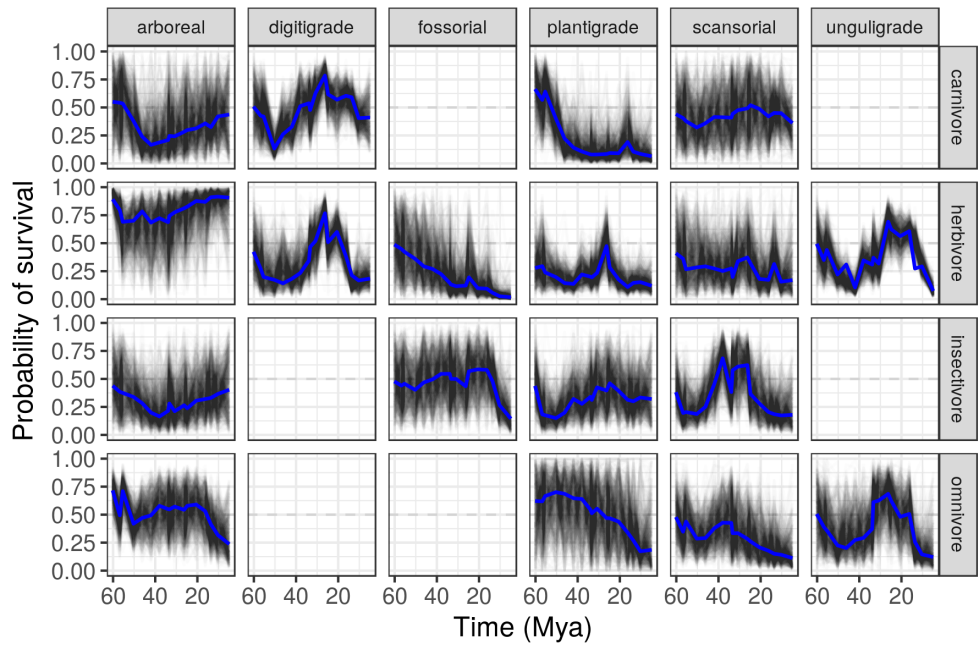


Figure 12: Probability of a mammal ecotype survival probabilities at each time point as estimated from the birth-death model. Each panel depicts 100 random samples from the model's posterior. The columns are by locomotor category and rows by dietary category; their intersections are the observed and analyzed ecotypes. Panels with no lines are ecotypes not observed in the dataset.

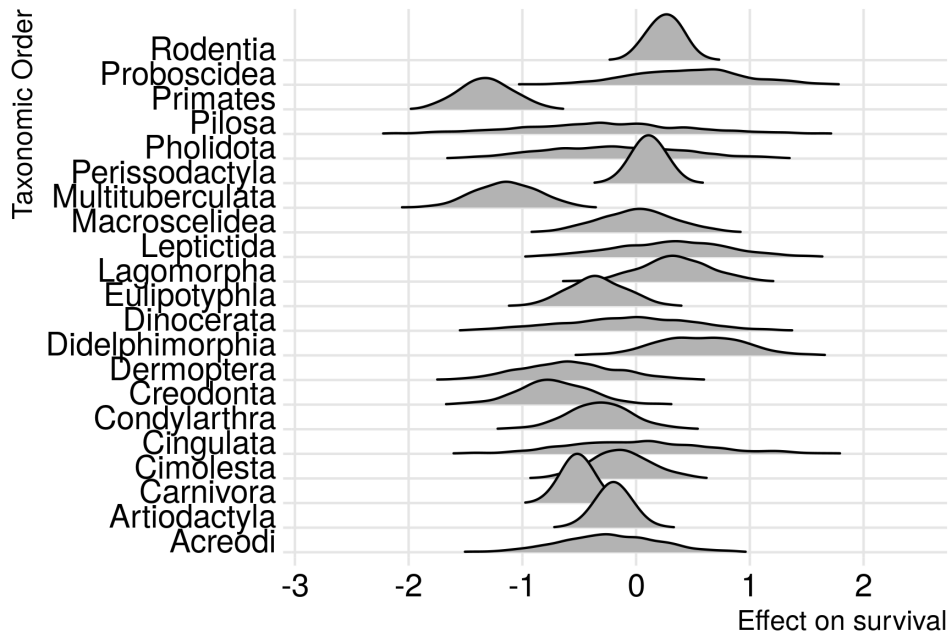


Figure 13

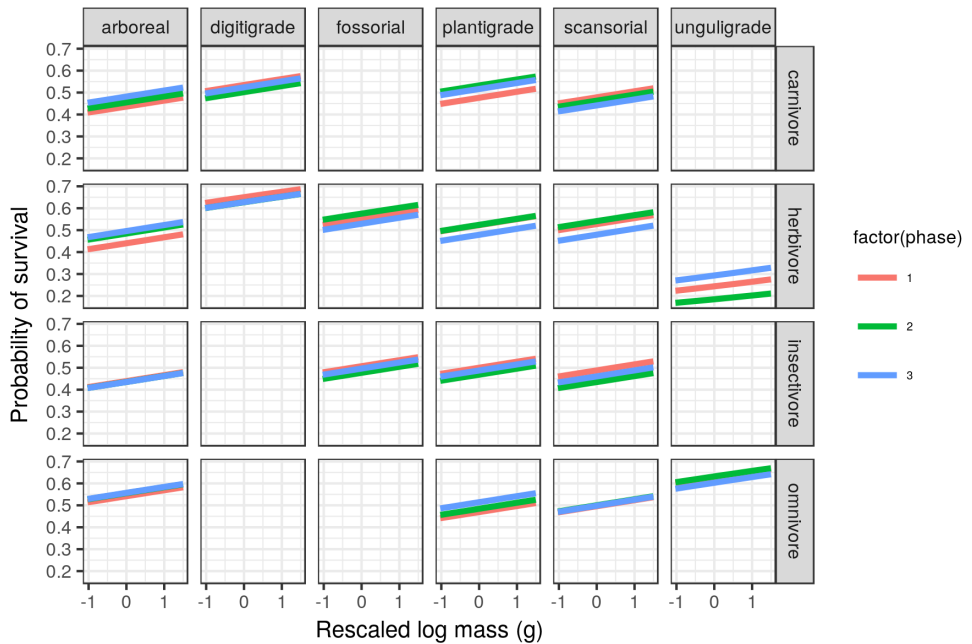


Figure 14: Mean estimate of the effect of species mass on the probability of a species survival for each of the three plant phases. The effect of mass is considered constant over time and that the only aspect of the model that changes with plant phase is the intercept of the relationship between mass and survival. The three plant phases are indicated by the color of the line. Mass has been log-transformed, centered, and rescaled; this means that a mass of 0 corresponds to the mean of log-mass of all observed species and that mass is in standard deviation units. For clarity, only the mean estimates of the effects of mass and plant plant are plotted.

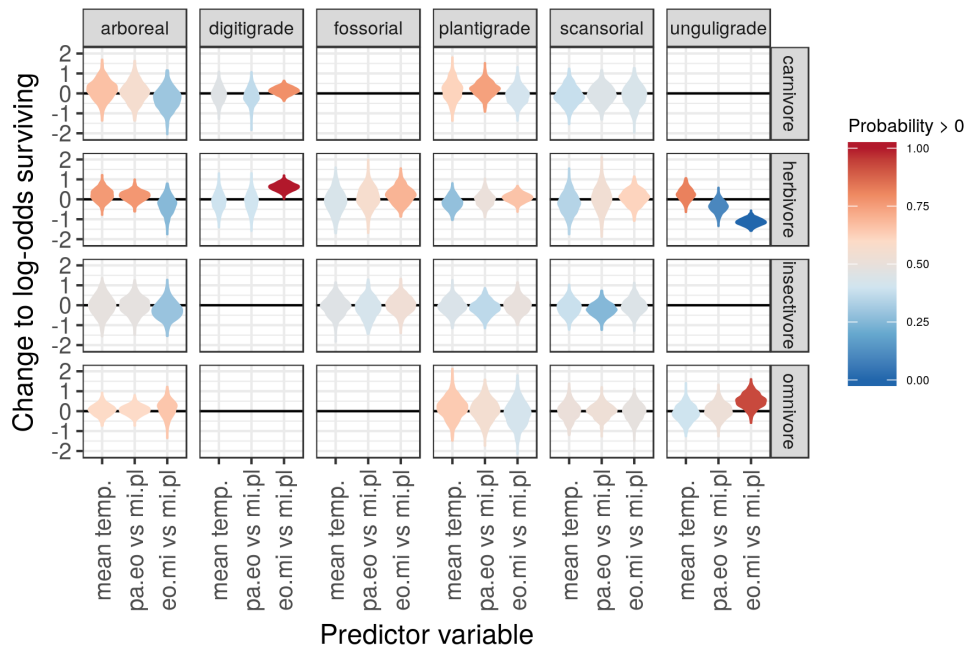


Figure 15: Estimated effects of the group-level covariates describing environmental context on log-odds of species survival. These estimates are from the birth-death model. What is plotted is a violin of the distribution of 1000 samples from the approximate posterior. The effect of plant phase graphed here is calculated as Phase 1 = $\gamma_{phase\ 1}$, Phase 2 = $\gamma_{phase\ 1} + \gamma_{phase\ 2}$, and so on.

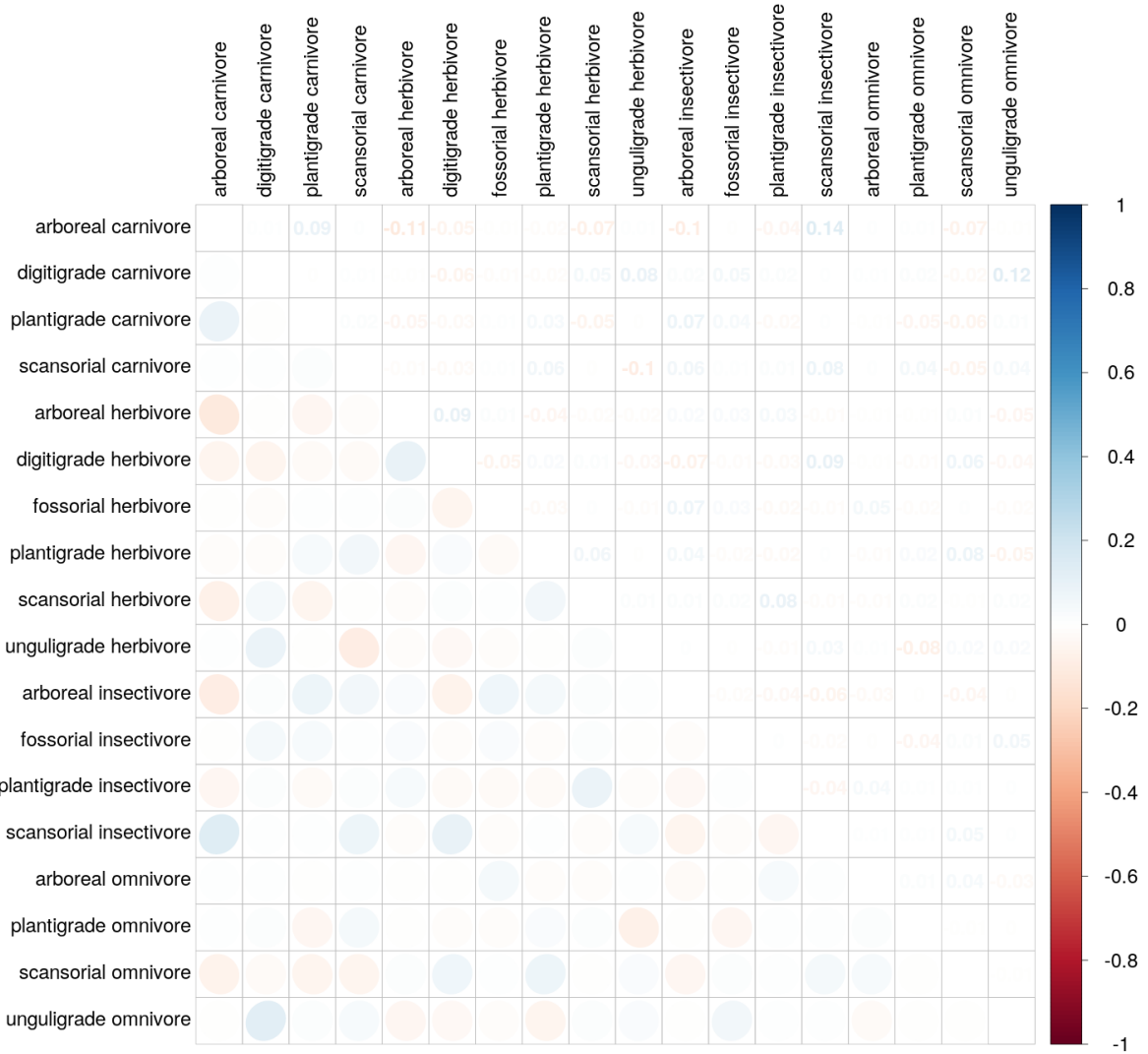


Figure 16: Posterior mean estimates of the correlations in survival probability between the mammal ecotypes. The lower triangle of the matrix is populated with ellipses corresponding to the level of correlation between the two ecotypes, while the upper triangle of the matrix corresponds to the mean estimated correlation between ecotypes. Darker values correspond to a greater magnitude of correlation with blue values corresponding to a positive correlation and red values a negative correlation.

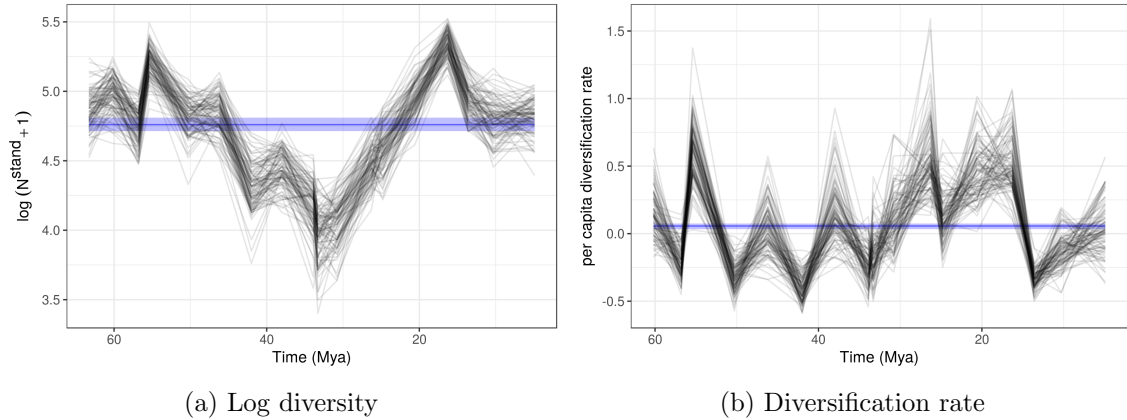


Figure 17: Posterior estimates of the time series of Cenozoic North American mammal diversity and its characteristic macroevolutionary rates; all estimates are from the birth-death model and 100 posterior draws are plotted to indicate the uncertainty in these estimates. The blue horizontal strip corresponds to the 80% credible interval of estimated mean standing diversity, diversification rate, origination rate, and extinction rate respectively; the median estimate is also indicated. What is also plotted is the The dramatic differences between diversity estimates at the first and second time points and the penultimate and last time points in this series are caused by well known edge effects in discrete-time birth-death models caused by $p_{-,t=1}$ and $p_{-,t=T}$ being partially unidentifiable (Royle and Dorazio, 2008); the hierarchical modeling strategy used here helps mitigate these effects but they are still present (Gelman et al., 2013; Royle and Dorazio, 2008). Diversification rate is in units of species gained per species present per time unit (2 My), origination rate is in units of species originating per species present per time unit, and extinction rate is in units of species becoming extinct per species present per time unit.

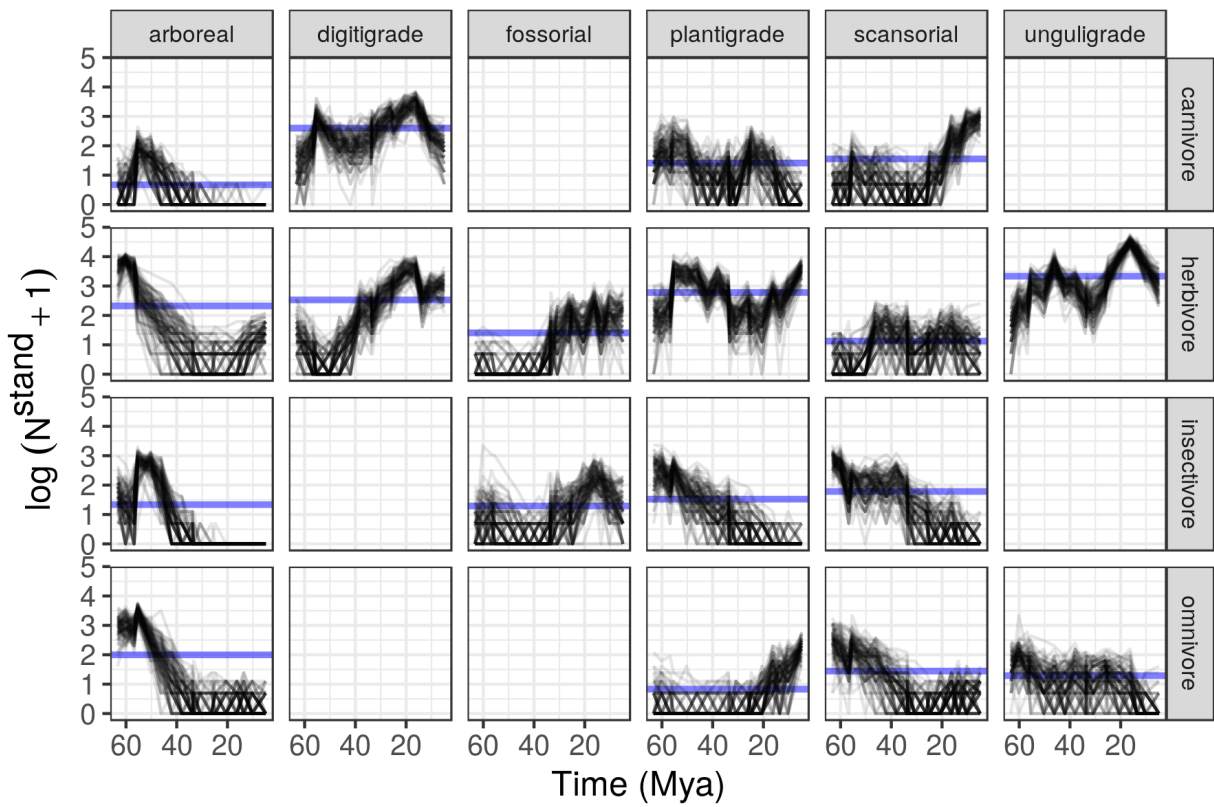


Figure 18: Posterior of standing log-diversity of North American mammals by ecotype for the Cenozoic as estimated from the birth-death model; 100 posterior draws are plotted to indicate the uncertainty in these estimates and what is technically plotted is \log of diversity plus 1.

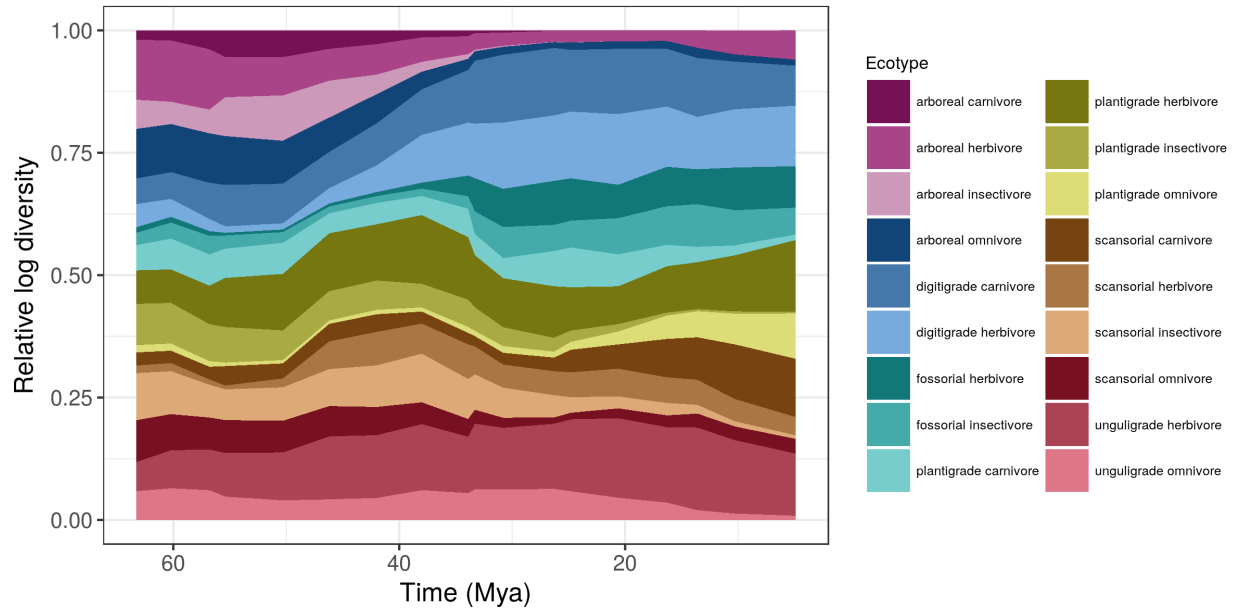


Figure 19: Mean posterior estimate of relative log standing diversity of 18 North American mammal ecotypes for the Cenozoic. These estimates are calculated from 100 posterior estimates of the true occurrence matrix z as estimated from the birth-death model.